The Effects of As-Cast Depth and Concrete Fluidity on Strand Bond

Robert J. Peterman, Ph.D., P.E.
Martin K. Eby Distinguished Professor
in Engineering
Kansas State University
Manhattan, Kans.

This paper presents the results from strand end-slip measurements and load tests of members that were fabricated at six different precast concrete plants over the past 2½ years. All of the work reported herein is based on specimens that were produced using standard concrete mixtures and placement techniques. As such, the data presented are believed to be representative of current industry practice.

This study revealed that the occurrence of the so-called top-bar effect (top-strand effect) for pretensioned strands is primarily a function of the amount of concrete above the strand rather than the amount of concrete below it. Accordingly, the results of this investigation indicate that the current design assumptions for bond in pretensioned members are unconservative for members with strands near the top (as-cast) surface. This phenomenon can result in extremely large transfer lengths for strands located within a few inches of the top surface, including those in thin members. In addition, the top-bar effect typically becomes more pronounced in members as concrete fluidity increases.

However, these same findings also revealed that the current design assumptions for bond were generally accurate when strands were located deeper in the members. This was true for members made with either flowable concrete or self-consolidating concrete.

In recent years, the use of self-consolidating concrete (SCC) has been increasing steadily among prestressed concrete producers in the United States. SCC is defined as a highly workable concrete that can flow through densely reinforced or geometrically complex structural elements under its own weight. It adequately fills voids without segregation or excessive bleeding and without the need for vibration.[1]

In 2004, the Precast/Prestressed Concrete Institute (PCI) co-funded an extensive investigation to evaluate the bond between SCC and prestressing steel in pretensioned concrete members. The PCI study had the following three objectives:

- Determine the ability of six currently used SCCs made with admixtures from each of four major admixture suppliers in the United States to meet current ACI[2] and AASHTO[3] requirements for

transfer and development length (see "Code Provisions for Bond in Pretensioned Members" on p. 76);

- Quantify the top-strand effect for pretensioned members made with SCC; and
- Develop a simple, industry-standard bond test for members made with SCC that precasters can readily conduct (this test will be described in detail in a future *PCI Journal* article).

This paper presents the findings of this study, which indicate that, in general, the assumption of a transfer length equal to $50d_b$ or $(f_{se}/3)d_b$ is largely unconservative for members with pretensioned strands located near the top (as-cast) surface, where d_b is the diameter of the strand and f_{se} is the effective stress in prestressed strand after all losses. The use of highly fluid concrete seems to exacerbate this effect.

BACKGROUND

In 2001, detailed information about the bond behavior of pretensioned strands in SCC was essentially absent from the literature. Because SCC does not require any external vibration during placement, many design engineers have questioned the ability of SCC to achieve adequate bond with smooth prestressing steel.

In 2002, the Kansas Department of Transportation (KDOT) funded an initial investigation to evaluate the bond between seven-wire pretensioned strand and SCC. In this initial study, large block pullout tests[18] (LBPTs) were performed at Kansas State University (KSU) using two different concrete mixtures. The first mixture was the standard concrete recommended by Logan,[18] and the second was an SCC that had been proposed for use in the state of Kansas (**Table 1**).

Concrete compressive strengths at the time of testing were 5600 psi (38.6 MPa) for the standard concrete and 6800 psi (49.6 MPa) for the proposed SCC. LBPT results with SCC had significantly lower first-slip and ultimate-load values compared with those values from the standard concrete tests (**Fig. 1**).

Table 1. Mixture Proportions for Concrete Used in Large Block Pullout Tests

	Logan Mix	SCC Mix
Cement (type 3)	660	750
Fine aggregate	1100	1500
Crushed gravel	1900	0
Limestone	0	1360
Type D water reducer & retarder	26	0
Type F HRWRA	0	70
Air-entraining admixture	0	5
Water	292	225
Water–cementitious materials ratio	0.44	0.30

Note: All values given in kilograms except for admixtures, which are shown in milliliters. HRWRA = high-range water reducing admixture; SCC = self-consolidating concrete. 1 mL = 0.0338 oz; 1 kg = 2.2 lb.

Logan recommended that 0.5-in.-diameter (13 mm) strand has an average minimum pullout capacity of 36 kip (160 kN) with a maximum coefficient of variation of 10% for a six-sample group. Logan has since recommended that the minimum average value of first-observed slip of 0.5-in.-diameter strand be 16 kip (71 kN).

Furthermore, the results from the LBPTs with SCC in 2002 were below the values of 16 kip (71 kN) and 36 kip (160 kN) for first-observed slip and maximum pullout force, respectively. Both LBPTs used strand from the same unweathered reel that had exhibited satisfactory bond performance in flexural beam tests. This strand is referred to as the control strand.

Based on the results from the LBPTs and similar findings from pullout tests conducted by other prestressed concrete producers in the United States (including High Concrete Structures Inc. and Stresscon Corp.), it appeared that the use of SCC can significantly reduce the bond capacity of untensioned strand cast in the vertical position, which would have direct design implications for all lifting devices that rely on friction. However, limited pretensioned (flexural) testing using SCCs at both Stresscon Corp. and KSU yielded satisfactory results. Thus, the ability of

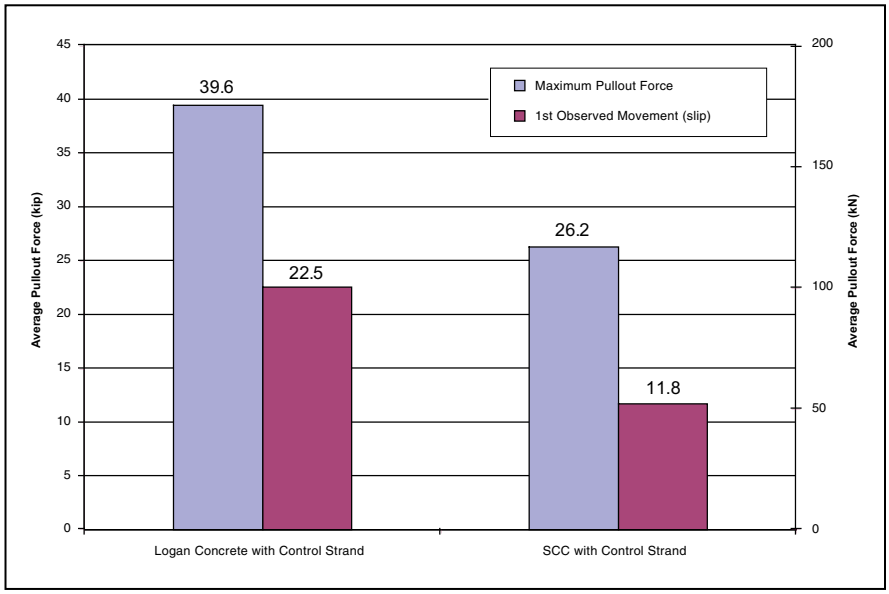

Fig. 1. Results from pullout tests with conventional concrete and self-consolidating concrete (SCC).

Table 2. Six SCC Mixes Used in This Study, yd³

		Mix 1	Mix 2	Mix 3	Mix 4	Mix 5	Mix 6
Continuous materials	Type 1 cement	600					
	Type 3 cement		700	602	700	584	750
	Slag	200				198	
	Class C fly ash		120		100		
	Class F fly ash			260			
	Water	306	321	290	295	332	308
	Water–cementitious materials ratio	0.38	0.39	0.34	0.37	0.42	0.41
Aggregates	Limestone	1461					1513
	River gravel			1433		1525	
	Lightweight				850		
	Granite		1635				
	Sand	1388	1100	1380	1248	1375	1422
	Sand-aggregate ratio	0.49	0.40	0.49	0.59	0.47	0.48
Admixtures	Type A water-reducing admixture						15
	Type D water reducer and retarder			43			
	Type F HRWRA	56	34	50	32	55	71
	AE	8	5.5		5.5	3	5.1
	Corrosion inhibitor	256				384	
	Admixture supplier	A	B	C	B	D	D

Note: All values are given in pounds except for admixtures, which are shown in ounces; AE = air-entraining admixture; HRWRA = high-range water-reducing admixture; SCC = self-consolidating concrete. 1 lb = 0.45 kg; 1 oz = 29.6 mL.

pretensioned members to meet current design assumptions for strand bond was uncertain.

EXPERIMENTAL PROGRAM

At the outset of this study, the project steering committee decided that the evaluated SCCs should represent the current mixtures used at PCI Producer Member plants. No mixtures were developed as part of this investigation. Thus, to achieve the objective of representing each of four different admixture suppliers, work was conducted at different precast concrete facilities throughout the United States.

This decision to fabricate specimens at different precast concrete facilities across the United States meant that there would be numerous variables introduced at each plant, including aggregate source, admixture types and dosages, mixer type, delivery vehicles, placement techniques, and curing methods. Evaluating the effect of individual producer components or procedures on bond was not a goal of the PCI study.

To maximize consistency among plants, the author and a doctoral student were present at each facility during casting to measure rheological properties and to perform all initial measurements of strand end slip. In addition, each plant produced identically sized specimens and used prestressing strand from the same reel.

Unweathered strand was set aside from a reel, and the required amount was sent to each of the precast concrete producers prior to casting. This strand was first prequalified for its bonding capability using the LBPT. In addition, a strand with lower bonding characteristics was purposely introduced to the study during the casting at one plant (mix 4) in order to determine the sensitivity of the specimen geometry used in this study.

As part of the experimental program, transfer length measurements were taken via the strand end-slip measurements of the bottom- and top-strand specimens. Due to an observed trend between transfer length and strand casting position, the project steering committee authorized more testing to determine the relationship between strand bond and casting position.

In an independently funded study, additional testing was performed on 4-in.-thick (100 mm) panels in two precast concrete plants, and end-slip measurements were gathered. Finally, a design approximation was developed from the gathered data.

Specimen Nomenclature

Specimens in this study were designated by a mix number, a letter, and a numerical description. The letter *B* is used to refer to the 10-

Table 3. Material Properties for the Six SCCs

Properties	Mix 1	Mix 2	Mix 3	Mix 4	Mix 5	Mix 6
Air content, %	6.4	4.0	1.0	6.0	7.9	3.5
L-box differential, *H2/H1*	0.93	0.76	0.95	0.76	0.93	1.00
Slump flow, in.	26	27	27 1/2	19 3/4	23 1/2	26
J-ring, in.	26	26	27	18	22 1/2	24 1/2
Visual stability index	0	0.5	0.5	0.5	0	0
Column segregation, *B/T*	1.00	0.58	0.66	0.93	1.08	0.91
Compressive strength at release, psi	3500	4560	3700	3600	5150	5830
28-day compressive strength, psi	8440	5970	10,170	6610	9230	10,760
28-day split tensile strength, psi	453	410	576	395	490	555
28-day modulus of elasticity, ksi	5255	2300	5200	3100	4300	5350

Note: B = bottom; T = top. 1 in. = 25.4 mm; 1 psi = 6.894 kPa; 1 ksi = 6.894 MPa.

in.-wide × 15-in.-deep (250 mm × 380 mm) specimens with a single strand cast 2 in. (50 mm) from the bottom of the specimen. Letter *T* refers to the 10-in.-wide × 15-in.-deep specimens with a single strand cast 2 in. from the top of the specimen. *SB* is used to refer to the 8-in.-wide × 6-in.-deep (200 mm × 150 mm) specimens. The designation *10* means that the specimen had an embedment length equal to the calculated ACI development length L_d, while the designation *08* implies that the specimen had an embedment length of only $0.80L_d$. This is the reason for the two 10-in.-wide beams of different lengths. All of the 8-in.-wide × 6-in.-deep SB specimens had embedment lengths equal to $0.80L_d$.

Evaluated SCCs, Material Properties

Table 2 shows the mixture proportions for each of the six SCCs evaluated in this study. It can be seen from this table that there is a large difference in the constituents and proportions of the different mixtures. Mixtures were developed by each of the precasting plants with their admixture suppliers. The precasting plants and mixtures chosen for evaluation in this study were selected by the admixture suppliers. Chosen plants had been producing SCC for more than one year and were believed (by the admixture suppliers) to best represent the current state of practice in the industry.

In Table 2, the four admixture suppliers are represented by the letters *A*, *B*, *C*, and *D*. In addition, each mixture is denoted by a number, rather than by the identity of the producer plant, to maintain the confidentiality of the participating organizations. One of the precasters produced both a normal-weight mixture and a lightweight mixture (mix 4). Thus, there was a total of six mixtures produced at five plants.

Table 3 lists the properties determined for each concrete. During placement, the following fresh concrete properties were measured and recorded: air content, slump flow (spread), visual stability index (VSI), J-ring, static (column) segregation, and L-box differential. In addition to the fresh concrete properties, the following hardened concrete properties were also determined: concrete compressive strength at release and at 28 days, modulus of elasticity (MOE), and split tensile strength.

From Table 3, it is clear that mix 4 was not truly an SCC because it had a spread of only 19 ¾ in. (500 mm). However, this was the standard mixture used by a precaster that was selected by its admixture supplier for inclusion in the SCC study.

Bottom-Strand Specimens

Six flexural (beam) specimens were cast with each of the six mixtures in order to evaluate the corresponding transfer and development lengths. As noted previously, the strand source was identical for all beams in this study except for the lower-bonding strand that was purposely introduced during the casting of mix 4 to determine the sensitivity of the specimen geometry.

These six specimens had two different rectangular cross sections. Five of the specimens had cross sections that were 10 in. (255 mm) wide × 15 in. (380 mm) deep. These beams were cast in two lengths, 11 ft 10 in. (3.6 m) and 9 ft 6 in. (2.9 m). The top (compression) width of 10 in. was selected so that the tensile strain in the strands at nominal moment capacity f_{ps} would exceed 3.5%, as recommended by Buckner.[11] A rectangular shape provided a relatively large width, thereby reducing the likelihood of shear failures in these specimens (they did not contain any stirrups). Both the project steering committee and external technical review committee did not want the strand bond in these members to be influenced by the presence of shear reinforcement. Thus, the specimens in this study contained only a single 1/2-in.-diameter (13 mm), 270 ksi (1860 MPa) prestressing strand.

In addition to the 10 in. × 15 in. (255 mm × 380 mm) rectangular specimens, one 8-in.-wide × 6-in.-deep (205 mm × 150 mm) specimen with an overall length of 9 ft 6 in. (2.9 m) was cast with each mixture. These specimens were tested as part of ongoing work to develop a simple strand bond test that can be conducted by precasters at their facilities.

(continued on page 78)

CODE PROVISIONS FOR BOND IN PRETENSIONED MEMBERS

Transfer length is the distance required to transfer the fully effective prestressing force from the strand to the concrete. Development length is the bond length required to anchor the strand as it resists external loads on a member.[4] As external loads are applied to a flexural member, the member resists the increased moment demand through increased internal tensile and compressive forces. This increased tension in the strand is achieved through bond with the surrounding concrete.[5]

Neither the American Concrete Institute's (ACI's) *Building Codes for Structural Concrete (ACI 318-05) and Commentary (ACI 318R-05)*[2] nor the fourth edition of the American Association of State Highway and Transporation Officials' *AASHTO LRFD Bridge Design Specifications*[3] require the use of a specific transfer length. However, ACI 318 suggests a transfer length of 50 strand diameters ($50d_b$) in section 11.4.4, while AASHTO suggests a value of $60d_b$ in section 5.11.4.

The expression for development length is found in ACI 318 section 12.9.1 and is shown in Eq. (1):

$$\text{Development length } L_d = f_{se}d_b/3 + (f_{ps} - f_{se})d_b \qquad (1)$$

where

d_b = diameter of strand (in.)

f_{se} = effective stress in prestressing strand after allowance of prestress losses (ksi)

f_{ps} = stress in prestressing strand at calculated ultimate capacity of section (ksi)

This expression suggests a transfer length $L_{tr} = f_{se}d_b/3$.

The AASHTO specifications have a similar expression for development length but require an additional 1.6 multiplier to Eq. (1) for precast, prestressed concrete beams with a depth greater than 24 in. (600 mm). However, instead of a suggested transfer length of $f_{se}d_b/3$, AASHTO Fig. C5.11.4.2-1 explicitly shows the transfer length to be $60d_b$ in the idealized bilinear depiction of strand stress variation.

Neither of the current ACI or AASHTO expressions for transfer or development length consider the casting position of the strand as a factor that influences the bond in pretensioned members. However, both of these documents consider the casting position of an untensioned deformed bar to be critical to the bond and corresponding development length.

ACI requires a 1.3 multiplier on development length of deformed bars for "horizontal reinforcement so placed that more than 12 inches (305 mm) of fresh concrete is cast in the member below the development length or splice."AASHTO requires a 1.4 multiplier for "top horizontal, or nearly horizontal reinforcement, so placed that more than 12.0 in. of fresh concrete is placed below the reinforcement."

The multipliers of 1.3 in ACI and 1.4 in AASHTO are used to address what is commonly referred to as the top-bar effect. Many researchers (Clark,[6,7] Menzel,[8] Ferguson and Thompson,[9] and Jirsa and Breen[10]) have documented that bars cast near the tops of deep members can have significantly longer development lengths than those bars cast near the bottoms of identical members. This effect has been attributed to the combined effects of bleed water and settlement.

When fresh concrete is placed, the excess (bleed) water and air tend to migrate upward toward the surface, thereby allowing the remaining concrete to settle (move downward). Because reinforcing bars are typically held in position by chairs or other supports, the settlement of the surrounding concrete acts to pull it away from the horizontal bars and the effect becomes more pronounced with increasing amounts of fresh concrete placed below the bars. In addition, the bottom surface of the solid bars provides a place for bleed water and air to become trapped, thereby causing a higher water–cementitious materials ratio and poorer consolidation of the paste in the immediate vicinity of the top bars.

In 1995, Buckner[11] recommended that that the development length be multiplied by a similar factor of 1.3 for any strands (straight or draped) that end in the upper one-third of the member depth and have 12 in. (305 mm) or more of concrete cast beneath them.

In 1996, Petrou and Joiner[12] reported on excessive slip that was occurring in strands located near the tops of pretensioned piles in South Carolina. The researchers experimentally determined that the strand transfer lengths were directly proportional to the extremely long end slips. In many instances, the amount of end slip for top strands was found to be two to three times the amount of end slip occurring for corresponding bottom strands in the same section. Additional documentation of this top-strand effect in piles was presented by Petrou et al.[13] and Wan et al.[14,15]

Wan et al.[14] noted that, in general, "as concrete slump increases, strand end slip increases." They recommended that "wherever practical, the slump of concrete mixtures used for prestressed concrete pile construction should be limited to 4 inches." The researchers also recommended that the use of a retarder should be avoided in pretensioned pile construction because "the presence of a retarder increases the top strand end slip while having little effect on the bottom strand slip." They further noted that the current practice of de-tensioning a member from the top down tended to increase the top-strand effect and recommended that the strands be de-tensioned in a symmetric manner, starting at the bottom of the pile.

In 1998, Lane[16] proposed a new development length equation that incorporated a 1.3 multiplier for strands that have 12 in. (300 mm) or more of concrete cast beneath them. A form of this equation was later adopted by the *AASHTO LRFD Bridge Design Specifications*[17] in section 5.11.4.2 with a 1.3 multiplier for top strand. However, this equation and the corresponding top-strand multiplier was removed in the next edition of the specifications.[3]

Table 4. Results from Load Tests to Failure

	Beam No.	Age at Test, days	Span, ft	Load at Failure, kip	Slip at Failure, in.	Moment at Failure M_{exp}, kip-ft	Calculated M_n, kip-ft	M_{exp} / M_n
Mix 1	B10R	27	11.5	16.33	<0.01	49.53	44.69	1.11
	T10R	28	11.5	16.32	<0.01	49.50	44.27	1.12
	B10F	36	11.5	16.48	<0.01	49.94	44.05	1.13
	SB	31	8.83	7.53	<0.01	17.12	13.70	1.25
	B08R	34	9.17	20.98	<0.01	49.73	39.30	1.27
	T08R	36	9.17	20.01	0.019	47.50	39.30	1.21
Mix 2	B10R	25	11.5	16.38	<0.01	49.62	43.73	1.13
	T10R	27	11.5	16.05	<0.01	48.71	43.48	1.12
	B10F	34	11.5	16.94	<0.01	49.53	43.19	1.15
	SB	29	9.17	6.24	0.200	15.95	12.70	1.26*
	B08R	32	9.17	21.23	<0.01	50.28	39.60	1.27
	T08R	35	9.17	20.70	0.011	47.45	38.80	1.22
Mix 3	B10R	26	11.5	16.30	<0.01	49.47	44.26	1.12
	T10R	28	11.5	16.17	0.013	49.01	43.80	1.12
	B10F	35	11.5	16.31	<0.01	49.48	43.93	1.13
	SB	32	9.17	6.16	<0.01	14.64	12.20	1.20
	B08R	35	9.17	21.20	<0.01	50.25	39.20	1.28
	T08R	37	9.17	20.99	<0.01	49.71	39.40	1.26
Mix 4	B10R	25	11.5	15.99	<0.01	48.01	42.47	1.13
	T10R	27	11.5	16.13	<0.01	48.40	43.31	1.12
	B10F	32	11.5	16.56	<0.01	49.69	43.34	1.15
	SB	30	9.17	6.28	<0.01	14.82	11.90	1.25*
	B08R	32	9.17	20.93	<0.01	49.32	39.00	1.26
	T08R	33	9.17	17.17	0.153	40.67	39.00	1.04*
	LB-SB	18	9.17	5.45	0.182	12.94	12.30	1.05*
	LB-B08R	24	9.17	19.02	0.087	44.89	37.90	1.18*
Mix 5	B10R	26	11.5	16.36	<0.01	49.58	44.57	1.11
	T10R	27	11.5	16.35	<0.01	47.79	43.93	1.09
	B10F	33	11.5	16.59	<0.01	50.14	44.58	1.12
	SB	27	9.17	6.35	<0.01	16.15	12.60	1.28
	B08R	30	9.17	20.50	<0.01	47.00	38.60	1.22
	T08R	32	9.17	20.72	<0.01	47.50	38.90	1.22
Mix 6	B10R	27	11.5	16.41	<0.01	49.68	44.14	1.13
	T10R	28	11.5	16.62	<0.01	48.58	43.29	1.12
	B10F	32	11.5	16.33	<0.01	49.47	43.28	1.14
	SB	29	9.17	5.64	0.034	14.54	13.30	1.09*
	B08R	32	9.17	20.87	<0.01	47.84	39.00	1.23
	T08R	33	9.17	20.23	0.203	46.38	39.00	1.19*

* Indicates failure in shear.

Note: 1 in. = 25.4 mm; 1 ft = 0.3048 m; 1 kip = 4.45 kN.

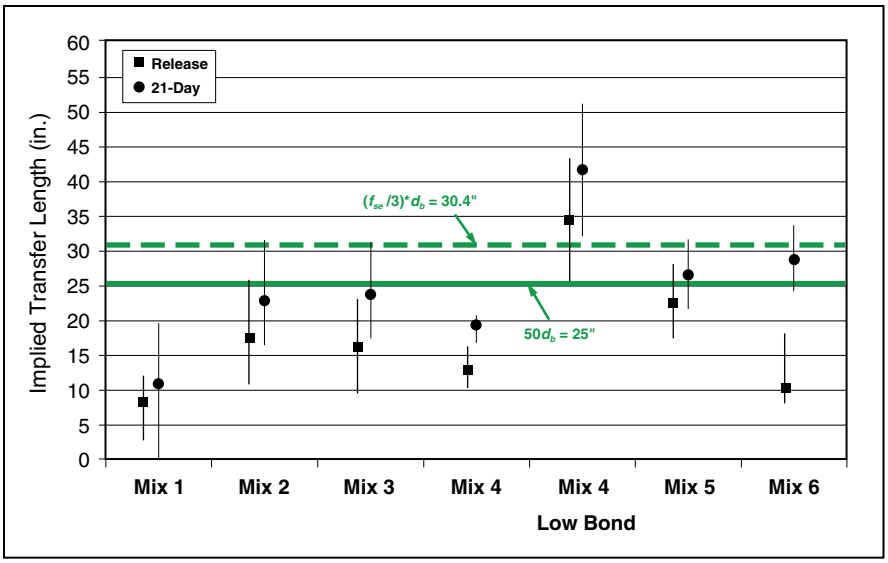

Fig. 2. Implied transfer lengths for 10 in. × 15 in. bottom strand beams. Note: " = inch. 1 in. = 25.4 mm.

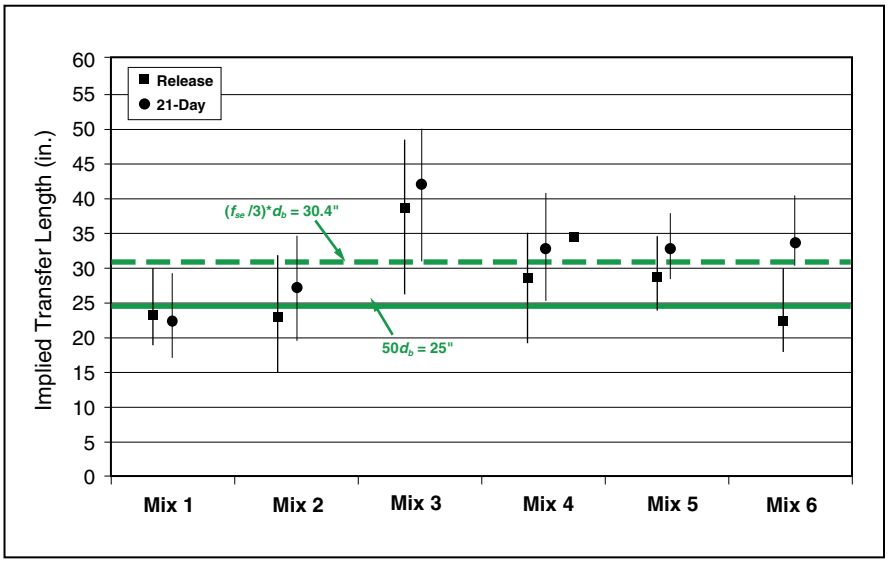

Fig. 3. Implied transfer lengths for 10 in. × 15 in. top strand beams. Note: " = inch. 1 in. = 25.4 mm.

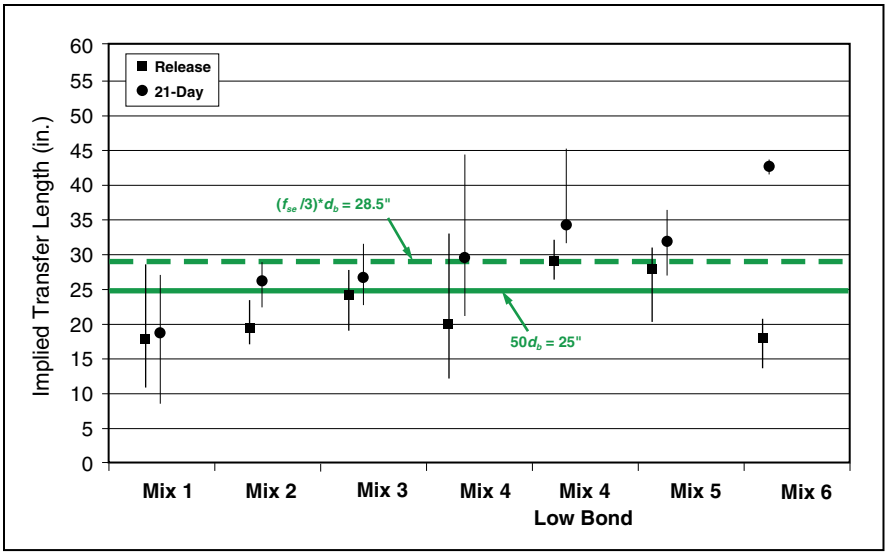

Fig. 4. Implied transfer lengths for 8 in. × 6 in. beams. Note: " = inch. 1 in. = 25.4 mm.

(continued from page 75)

Top-Strand Specimens

In three of these specimens, the strand was centered 2 in. (50 mm) from the bottom and had a corresponding depth from the top of 13 in. (330 mm). In the other two specimens, the strand was cast with a strand depth from the top surface of only 2 in. and a corresponding distance from the bottom of 13 in. These two companion specimens were used to quantify the top-strand effect for strand in SCC, where 12 in. (300 mm) or more of concrete was cast below the strand.

Load Test Results

Each of the 38 specimens (six specimens per each of six SCCs with the project strand plus two specimens with mix 4 and a low-bonding strand) was able to withstand the calculated ACI nominal moment capacity when loaded to failure in center-point bending. These specimens were tested after they achieved their design compressive strength f_c' and within 38 days of casting. This was done to investigate the perceived worst-cast scenario in which the precast concrete product would be erected and loaded at an early age. Nominal moment capacities were calculated using strain compatibility, considering the as-built dimensions of each specimen and the actual concrete compressive strength.

During specimen loading, the load, midspan deflection, and strand slip at each end were continuously monitored and recorded using a Keithley 20-bit data acquisition system. **Table 4** lists the results from each load test, including the strand end slip occurring at the maximum load and the corresponding moment achieved. In each case, the experimental moment exceeded the calculated ACI nominal moment capacity. In most cases, the ultimate failure was by rupture of the strand in tension. All other specimens failed in bond/shear, except mix 4 SB, which failed in shear. These failure modes are indicated by an asterisk in the column titled M_{exp}/M_n.

The two specimens that incorporated the lower-bonding strand, and which had considerably higher strand end-

slip values, were still able to achieve the ACI nominal moment capacity. Both of these specimens failed in bond/shear. Because all of the specimens in this study were tested at an early age, it is uncertain whether the strand in these two specimens would have undergone additional slip with age, resulting in a reduced long-term capacity. Furthermore, while several of the members in this study had 21-day implied transfer lengths that were longer than those assumed by the ACI code, these members were still able to withstand the ACI nominal moment capacity when loaded to failure.

RESULTS FROM ORIGINAL TRANSFER-LENGTH MEASUREMENTS IN SCC

Figures 2 through **4** show the transfer lengths, implied from strand end-slip measurements, for the three different specimen types (see "Estimating Transfer Length from Strand End-Slip Values" on p. 87). In each of these figures, the average implied transfer length at release is denoted by a square, with a vertical bar representing the range of values obtained for the different specimen ends measured. Transfer-length values measured after 21 days are denoted in a similar manner but with a circle representing the average value.

Figure 2 shows that the average transfer length for the 10-in.-wide × 15-in.-deep (255 mm × 380 mm) bottom-strand specimens was shorter than $(f_{se}/3)d_b$ for all six SCCs (when using the project strand that was prequalified for bond using the LBPT procedure[18]). When the lower-bonding strand was introduced, strand end-slip values and the corresponding transfer lengths more than doubled. In these cases, the transfer lengths at release and at 21 days were clearly longer than the values assumed by ACI methods. This indicates that the sizes of the specimens used in this study made the specimens sensitive enough to detect potential bonding problems.

Figure 3 shows the implied transfer-length results for the 10-in.-wide × 15-in.-deep (255 mm × 380 mm) top-strand specimens. For the top-strand

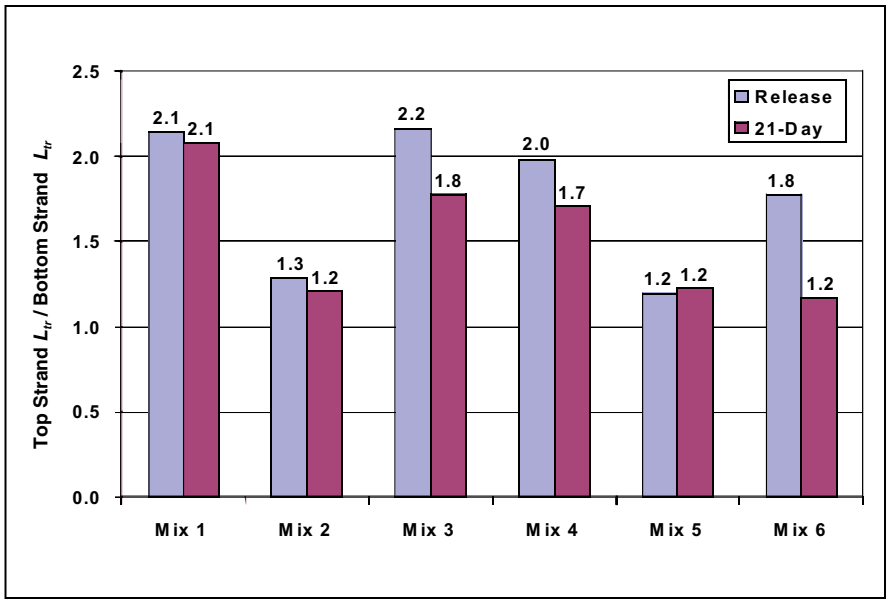

Fig. 5. Effect of strand casting position on implied transfer lengths.

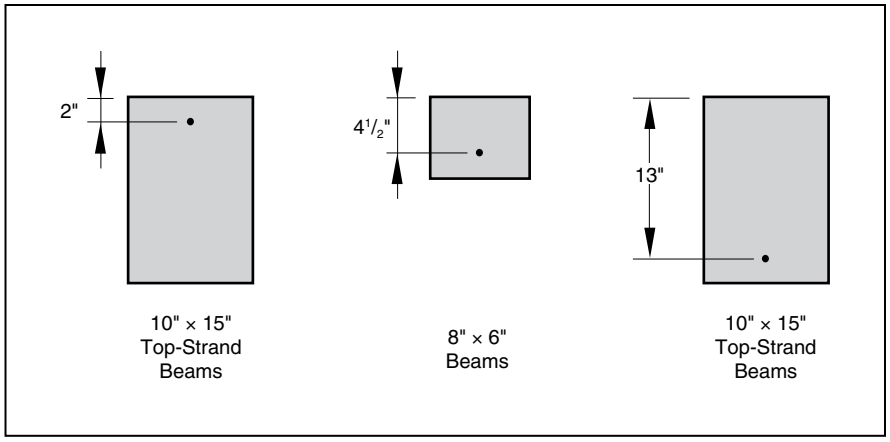

Fig. 6. As-cast strand depth of each member type. Note: " = inch. 1 in. = 25.4 mm.

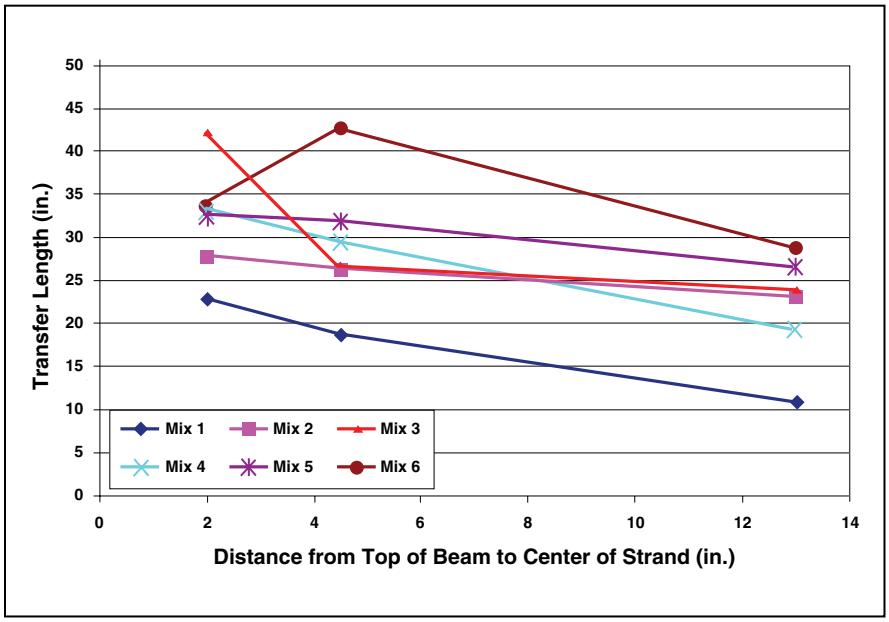

Fig. 7. Implied transfer length versus as-cast strand depth. Note: 1 in. = 25.4 mm.

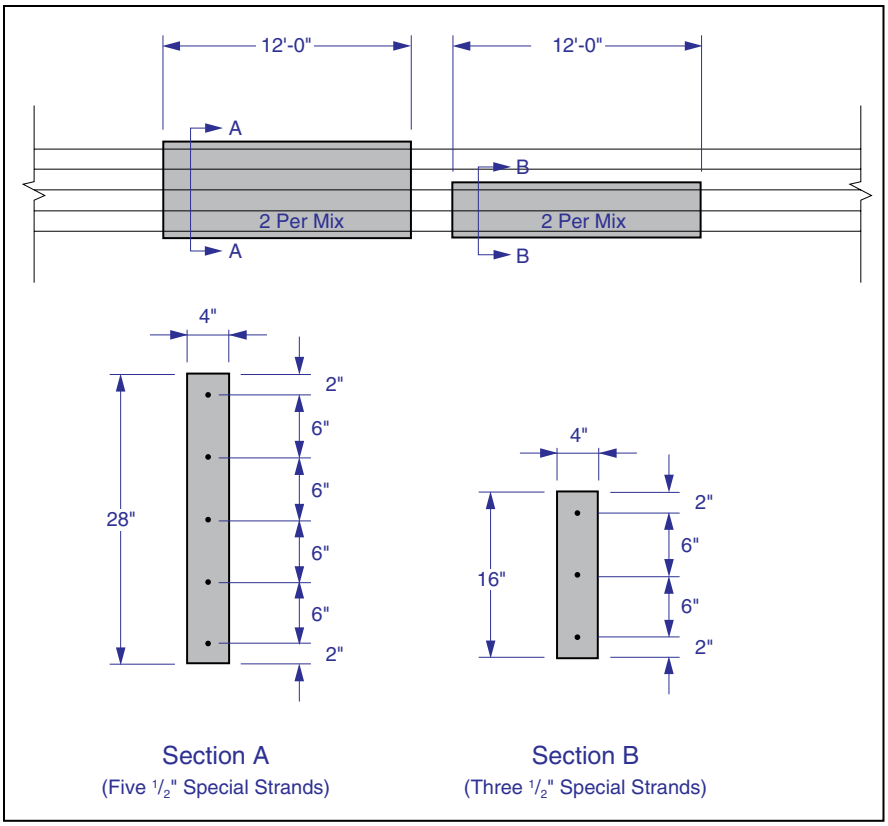

Fig. 8. Specimens used to de-couple the effect of strand placement on transfer length. Note: " = inch; ' = foot. 1 in. = 25.4 mm; 1 ft = 0.3048 m.

specimens, the average transfer lengths at 21 days for four of the six mixtures (mix 3 through 6) were longer than the ACI-assumed value of $(f_{se}/3)d_b$ when the prequalified project strand was used. In the top-strand beams, the average 21-day transfer length of all six mixtures was nearly 30% longer than the assumed value of $50d_b$. The lower-bonding strand was not used in any of the top-strand beams.

Mix 3 had the highest implied transfer lengths for the top-strand beams. The average 21-day transfer length for this mixture was nearly 70% longer than $50d_b$ and nearly 40% longer than $(f_{se}/3)d_b$. Mix 3 was the only one that contained a retarding admixture (Table 2). Wan et al.[14] noted that the use of a retarding admixture increased the top-bar effect in pretensioned piles.

Mix 3 also had the second largest amount of column segregation (B/T = 0.66) (Table 3). Mix 2, however, had the largest amount of column segregation (B/T = 0.58) yet had the second lowest average implied transfer lengths at 21 days of all top-strand beams. By examining Table 3 and **Fig. 2, 3**, and **5**, it is evident that none of the rheological properties measured during the casting of the six mixtures showed consistent correlation with the corresponding strand end-slip measurements and implied transfer lengths.

Figure 5 compares the average transfer lengths L_{tr} of the top-strand beams with those of the bottom-strand beams for each mixture. From this figure, a significant reduction in bond associated with the strand casting position for all six mixtures is evident, with the largest initial ratio occurring for mix 3. In the top-strand beams, there was only 2 in. (50 mm) of concrete above the center of the strand at the time of casting. However, this figure can be somewhat misleading if viewed independently from Fig. 2 and 3. Figure 5 indicates that mix 1 has a large 2.1 top-strand ratio (the ratio of implied transfer lengths for top-cast versus bottom-cast strands), yet this mixture had the lowest total 21-day average transfer lengths of the top-strand beams (Fig. 3).

Figures 2 through 4 indicate that there was typically an increase in strand end slip and, therefore, implied transfer lengths during the first 21 days after de-tensioning. This increase averaged 36.3% for the bottom-strand beams, 15.8% for the top-strand beams, and 26.7% for the smaller, 8 in. × 6 in. (205 mm × 150 mm) beams. These values are somewhat larger than the 10% to 20% typical increase reported by Barnes et al.[22] and Oh and Kim[23] for pretensioned concrete members.

Observed Dependence of Transfer Length on Strand Casting Position

While it is apparent (from Fig. 5) that the strand casting position can have a significant effect on pretensioned strand bond, it is not clear from the data presented whether the effect is primarily due to the amount of concrete below the strand (as implied by the ACI requirement of a 1.3 multiplier for deformed bars with more than 12 in. [300 mm] of concrete below the bar), the lack of concrete above the strand, or a combination of both. In Fig. 2 through 4, the author noted that the implied transfer lengths for the 8 in. × 6 in. (205 mm × 150 mm) rectangular beams (Fig. 4) were generally between the corresponding values for the 10 in. × 15 in. (255 mm × 380 mm) beams with top and bottom strands.

Thus, the author plotted the average implied transfer lengths of each SCC as a function of strand depth from the top of the member. These depths are depicted in **Fig. 6** for each member type, with the corresponding plot shown in **Fig. 7**. With the exception of mix 6, there is a general trend of increasing transfer lengths (decrease in bond) with a reduction of the strand depth in the as-cast position.

The author presented this observed trend in October 2005 at the PCI Convention in Palm Springs, Calif. As a result of these preliminary findings, the project steering committee authorized additional testing on both conventional concrete and high-fluidity concrete to determine the effect of casting position on bond in pretensioned members.

ADDITIONAL TESTING INVESTIGATES STRAND BOND, CASTING POSITION

In June 2006, the author returned to two of the precasting plants involved in the first round of SCC testing to con-

Table 5. Concrete Mix Proportions for Addition Test Series

		Mix 1*		Mix 2*		Mix 4*	
		Conventional	SCC	Conventional	Flowable	Conventional	Flowable
Cementitious materials	Type 3 cement	562	600	700	700	700	700
	Slag	188	150				
	Class C fly ash			120	120	100	100
	Water	285	285	290	290	295	295
	Water–cementitious materials ratio	0.38	0.38	0.35	0.35	0.37	0.37
Aggregates	Limestone	1740	1500				
	Lightweight					850	850
	Granite			1635	1635		
	Sand	1185	1368	1100	1100	1248	1248
Admixtures	Type B, D water reducer and retarder					16	16
	Type D water reducer and retarder	10					
	Type A, B, D water reducer and retarder					24	24
	Type F HRWRA	65	45	28	35	28	35
	AE	12.0	6.0	7.0	7.0	7.0	7.0
	Type C accelerator	75					
	Admixture supplier	A	A	B	B	B	B

Note: All values are given in pounds per cubic yard except for admixtures, which are shown in fluid ounces; AE = air-entraining admixture; HRWRA = high-range water-reducing admixture. 1 lb/y^3 = 0.593 kg/m^3; 1 oz = 29.6 mL

duct strand end-slip measurements on specimens with varying strand heights and concrete fluidities. These test specimens were specifically designed to decouple the effects of strand height from the top and bottom of the specimen. Both high-fluidity and conventional concrete mixtures were investigated to determine whether the noted effect was unique to high-fluidity concrete.

Figure 8 depicts the specimens used in this additional test series. These specimens had widths of only 4 in. (100 mm) to address concerns that specimens in the original test program contained too much confining concrete around the strand. A total of five ½ in. (13 mm) special diameter strands, initially tensioned to $0.75f_{pu}$, were used for the fabrication of these test specimens. The 28-in.-high (710 mm) specimens contained five strands, while the

Fig. 9. Transition point between a 28-in.-tall specimen and a 16-in.-tall specimen. Note: 1 in. = 25.4 mm.

Table 6. Concrete Properties for Additional Mixes

Properties	Mix 1*		Mix 2*		Mix 4*	
	Conventional	SCC	Conventional	Flowable	Conventional	Flowable
Air content, %	5.6	5.2	4.8	4.3	4.5	6.3
Spread or slump flow, in.	$7^1/_2$	$23^1/_2$	$6^3/_8$	$18^3/_4$	$3^1/_2$	$19^3/_4$
Visual stability index	0.0	0.0	0.0	0.0	0.0	0.0
Concrete temperature, ˚F	73	71	93	92	91	93
Compressive strength at release, psi	3460	3460	4620	3940	4570	3940
28-day compressive strength, psi	8620	8940	7470	6140	8510	7010

Note: 1 in. = 25.4 mm; 1 psi = 6.894 kPa; ˚C = (˚F - 32)/1.8.

16-in.-high (410 mm) specimens contained only three strands (**Fig. 9**). The same single reel of prestressing strand that qualified for bond using the LBPT procedure[18] was shipped between the two different prestressing plants that were producing test specimens. De-tensioning was achieved by flame cutting with a torch to ensure sudden release.

The section heights were selected so that the implied transfer lengths of the three strands in the 16-in.-deep (410 mm) specimens could be directly compared with those from companion strands in the 28-in.-deep (710 mm) section. The top three strands in the 28-in.-deep section had the same amount of fresh concrete cast above them as those in the 16-in.-deep section, while the bottom three strands in the 28-in.-deep section had exactly the same amount of fresh concrete cast below them.

The author evaluated a total of six mixtures in this series: three mixtures with high concrete fluidity (flowable concrete or SCC) and three corresponding mixtures with the same coarse aggregate but with a targeted slump of 6 in. (150 mm). Two 28-in.-deep (710 mm) and two 16-in.-deep (410 mm) specimens were cast for each mixture. Thus, there were typically four end-slip measurements for each unique combination of strand location (fresh concrete depth above and below) and concrete type.

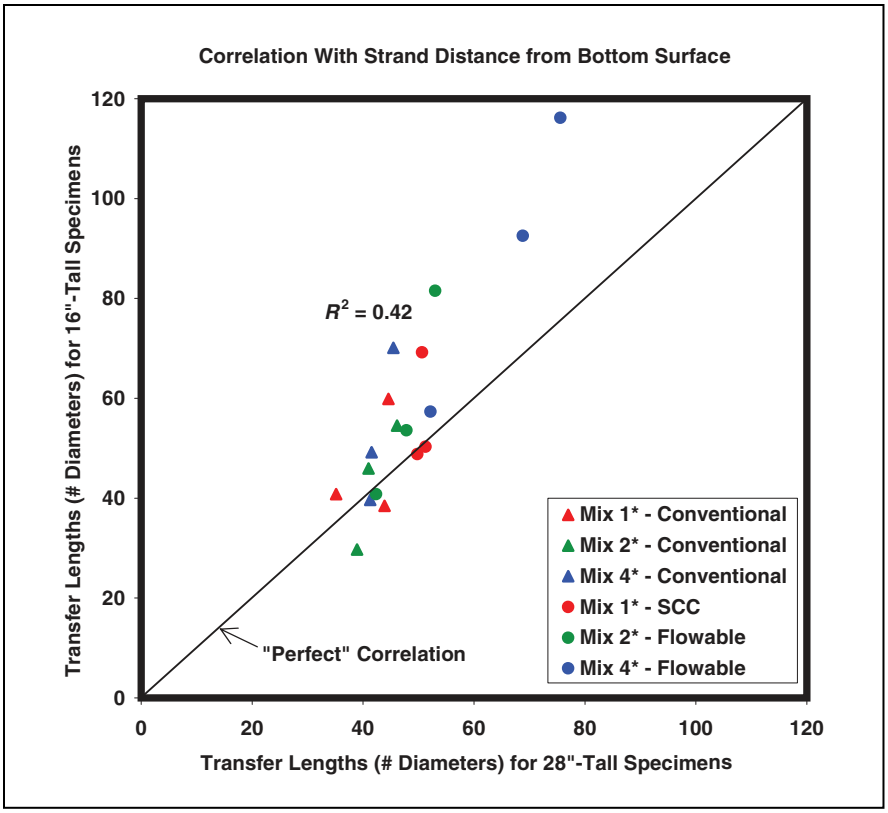

Fig. 10. Correlation of transfer lengths with strand distance from bottom surface. Note: SCC = self-consolidating concrete; " = inch. 1 in. = 25.4 mm.

Table 5 shows each of the six mixtures used in this test series. Each mixture series is designated by a number and an asterisk. The mixture number corresponds to the same coarse and fine aggregates used in the initial PCI test series. In fact, the SCC and flowable mixtures in the additional test series were similar to those in the original SCC test series. However, the mixtures denoted as conventional were standard mixtures that were previously used by the plants in production (before employing the currently used high-fluidity mixtures). Mix 2* and 4* were cast at the same prestressing plant. Mix 4* was a lightweight mixture.

Although a target slump of 6 in. (150 mm) was selected for the conventional mixtures, actual slumps ranged from $3^1/_2$ in. (89 mm) for mix 4* conventional to $7^1/_2$ in. (191 mm) for mix 1* conventional.

Table 6 lists the material properties of each of the mixtures. For this test series, only the consistency (spread or slump), visual stability, air content, and temperature were measured at the time of casting.

It is important to note that no vibration was used during the placement of the high-fluidity mix 1* because it was an SCC. However, internal vibration was used during the placement of the flowable mixtures (mix 2* and 4*) because they did not have a slump flow of at least 23 in. (580 mm). All specimens with the conventional concrete were internally vibrated during casting.

Results from Additional De-coupling Tests

Figure 10 shows the average implied transfer lengths, after 90 days, of the strands from the 16-in.-tall (410 mm) specimens plotted versus the average transfer lengths from the corresponding strands in the 28-in.-tall (710 mm) specimens (the same amount of fresh concrete cast below). The coefficient of determination R^2 for these data points with respect to the theoretical line of perfect correlation is only 0.42.

However, **Fig. 11** graphs these same average implied transfer lengths from the 16-in.-tall (410 mm) specimens versus the corresponding transfer lengths from the top three strands in the 28-in.-high (710 mm) specimens (with the same amount of fresh concrete cast above). In this plot, the coefficient of determination R^2 is 0.83. This means that 83% of the variation in average transfer lengths between different-height specimens with the same concrete can be predicted by the variation in the amount of fresh concrete cast above the center position of the strands. This indicates that the primary variable contributing to the observed top-strand effect is the amount of fresh concrete cast above the strands.

In **Fig. 12**, it can also be seen that a majority of the data points lie just below the line of perfect correlation, meaning that in general, the transfer lengths of the strands in the 28-in.-high (710 mm) specimens were slightly longer that those for the 16-in.-high (410 mm) specimens with the same amount of fresh concrete cast above. This is likely due to the corresponding—top three—strands in the 28-in.-high specimens having a larger amount of concrete cast below them. Thus, it is plausible that the amount of fresh concrete cast below the strands is a contributing factor to the observed top-strand effect, but it is clearly not the primary factor (as established by the low R^2 value in Fig. 11).

A better correlation of average transfer lengths with fresh concrete cast above the strands can be observed by comparing the six graphs of transfer length with these corresponding top and bottom distances. Compare Fig. 12 with **Fig. 13**, **Fig. 14** with **Fig. 15**, and **Fig. 16** with **Fig. 17**. Figures 16 and 17 show the transfer lengths for mix 4* corresponding to the mixtures with lightweight aggregate. The transfer lengths corresponding to the mixtures with lightweight aggregate were significantly longer than those resulting from mixtures with normalweight aggregate (mix 1* and 2*).

Figures 13, 15, and 17 show the transfer length increases with strand proximity to the top surface. This effect became more pronounced, especially for the uppermost strand, when the concrete fluidity was increased. Thus, all three mixtures exhibited a consistent

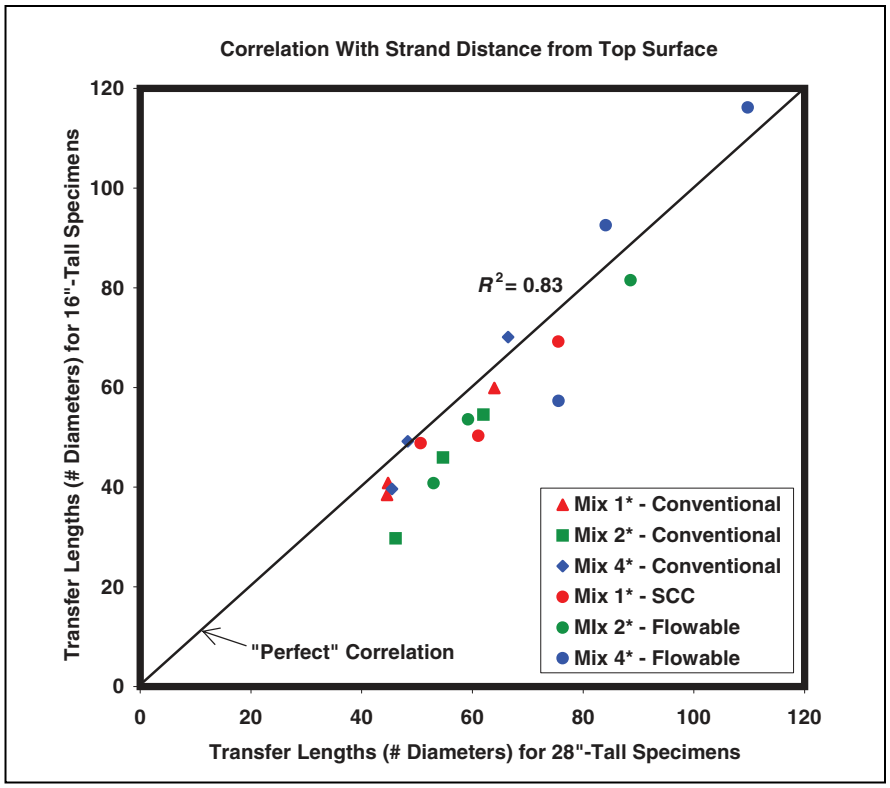

Fig. 11. Correlation of transfer lengths with strand distance from top surface. Note: SCC = self-consolidating concrete; " = inch. 1 in. = 25.4 mm.

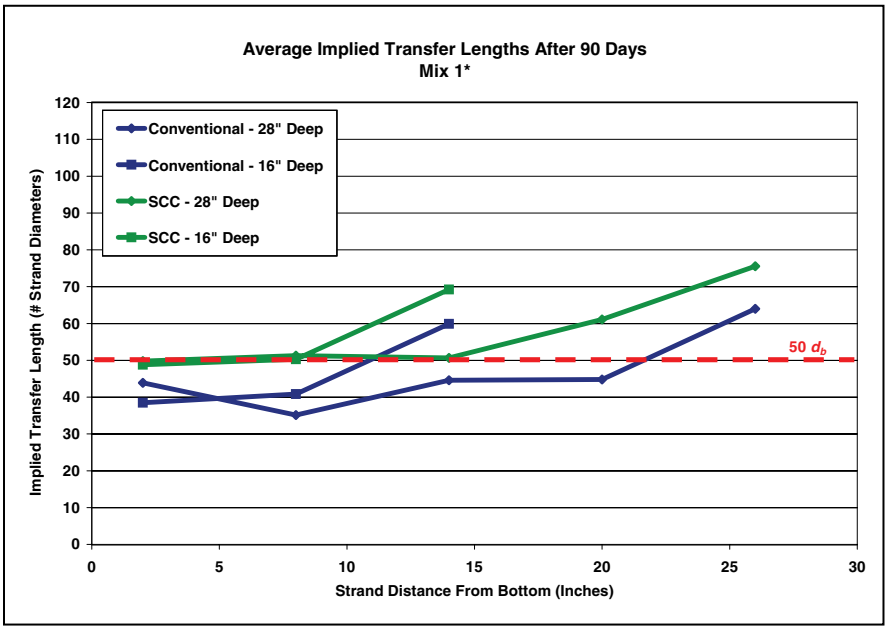

Fig. 12. Transfer lengths of mix 1* versus strand distance from bottom. Note: SCC = self-consolidating concrete; " = inch. 1 in. = 25.4 mm.

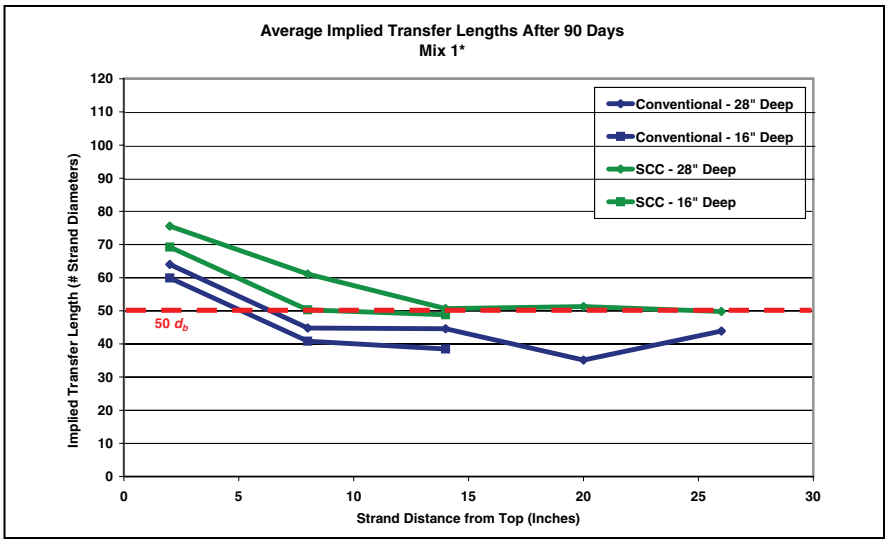

Fig. 13. Transfer lengths of mix 1* versus strand distance from top. Note: SCC = self-consolidating concrete. " = inch. 1 in. = 25.4 mm.

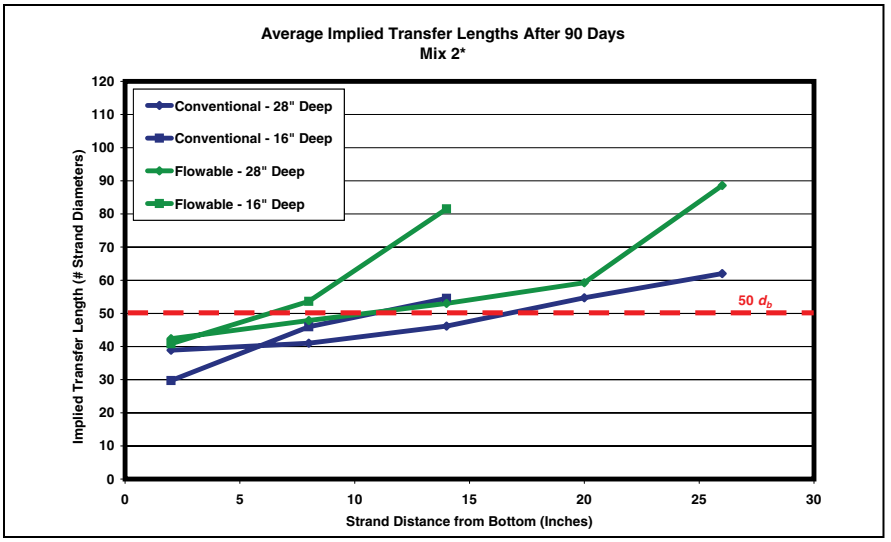

Fig. 14. Transfer lengths of mix 2* versus strand distance from bottom. Note: " = inch. 1 in. = 25.4 mm.

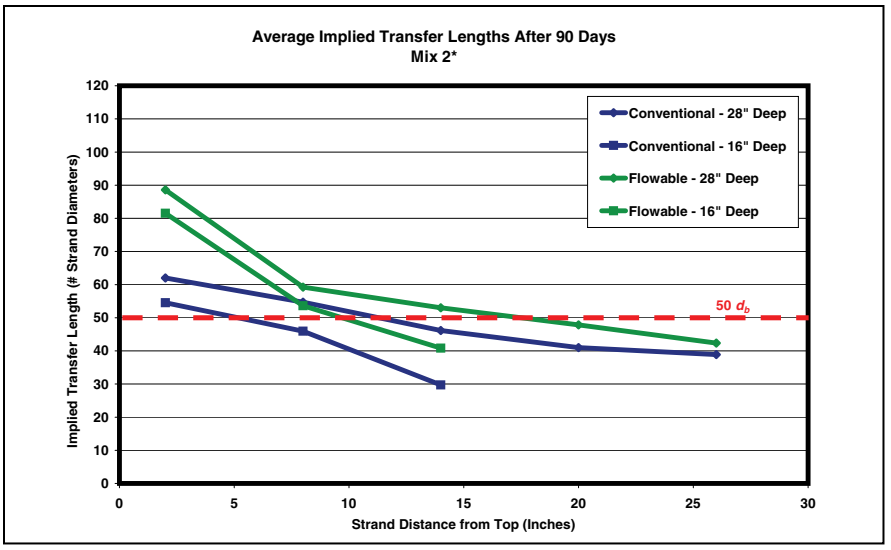

Fig. 15. Transfer lengths of mix 2* versus strand distance from top. Note: " = inch. 1 in. = 25.4 mm.

trend: when fluidity is increased while holding the water–cementitious materials ratio constant, the bond between the concrete and prestressing steel was significantly reduced.

ADDITIONAL STRAND END-SLIP TESTS

After observing a significant reduction in bond capacity near the top (as-cast) surface of pretensioned members, especially when high-fluidity concrete was used, it became apparent that there could be some significant design implications for standard pretensioned products, especially shallow members. Therefore, engineering managers at two different PCI member plants asked the author to determine strand end-slip values and corresponding implied transfer lengths of standard members in production at their plants.

In April 2006, the author measured strand end slips on members of various shapes at a PCI Producer plant (plant A). This particular precasting plant utilized a flowable concrete for the majority of its structural members, with a typical slump flow (spread) from 17 in. to 21 in. (430 mm to 530 mm). This precaster typically measures the spread, instead of slump, of its flowable concrete to better determine variations in consistency and thereby improve quality control. A concrete slump flow from 17 in. to 21 in. is analogous to a slump of approximately 9½ in. to 10 in. (240 mm to 250 mm). All concrete placements at plant A were consolidated using handheld, shaft-type vibrators.

As part of the assessment program at plant A, strand end-slip measurements were made by grinding a notch and then using a digital measuring device with positive interlock on several different types of members, including rectangular beams, L-beams, 4-in.-thick (100 mm) panels, and 6-in.-thick (150 mm) panels (**Fig. 18–20**). These product types were all cast using standard, normalweight, flowable concrete. **Table 7** lists each member type, the date the member was de-tensioned, the concrete unit weight, air content, spread, VSI, and the concrete strength prior to de-tensioning. Prior to de-tensioning, the form bulkheads were re-

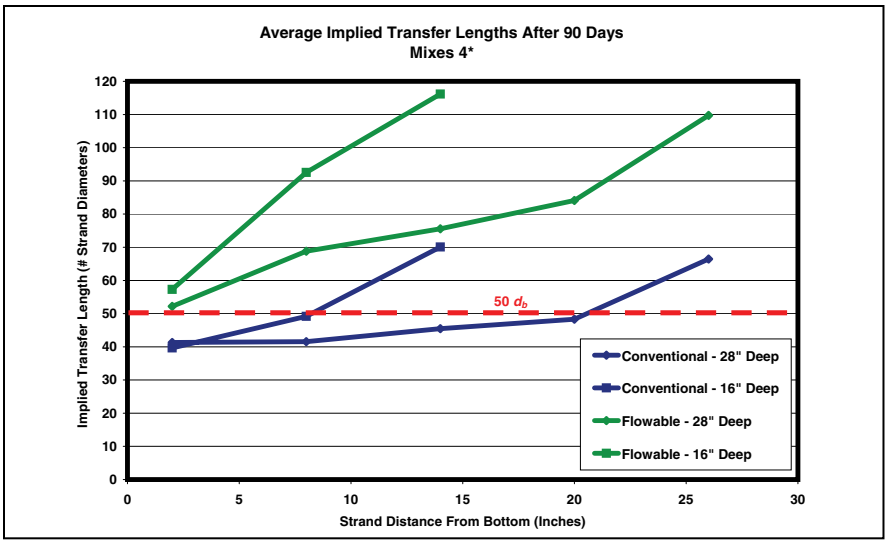

Fig. 16. Transfer lengths of mix 4* versus strand distance from bottom. Note: " = inch. 1 in. = 25.4 mm.

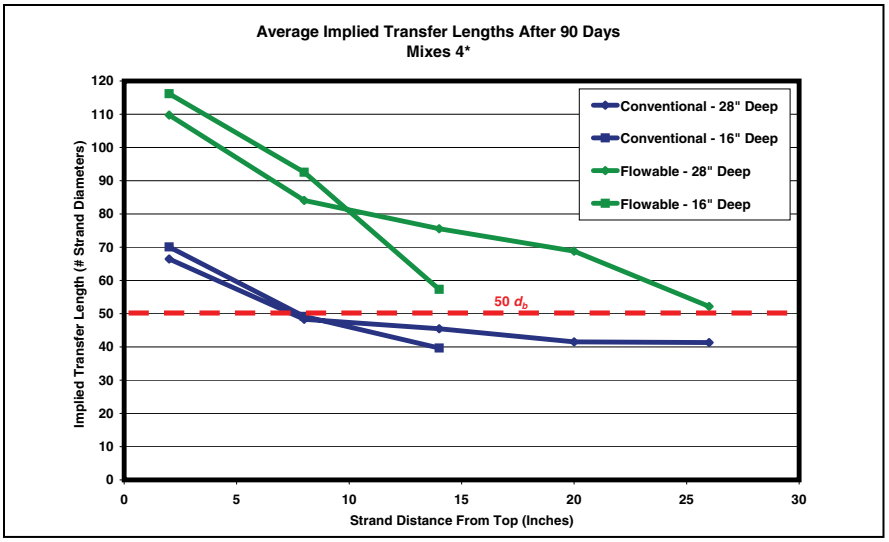

Fig. 17. Transfer lengths of mix 4* versus strand distance from top. Note: " = inch. 1 in. = 25.4 mm.

moved and the concrete was cleaned to allow for direct measurements with respect to the member end. In all cases, de-tensioning was accomplished by heating with a torch.

All of the plant A measurements reported in this paper utilized $^1/_2$ in. special-diameter (13 mm) strands. Samples were cut from one of the strand reels used in the member production, and LBPTs were later performed. These LBPTs revealed that the strand met the equivalent bond stress requirements recommended by Logan.[18]

If initial losses are assumed to be about 6% (with a corresponding f_{si} of about 190 ksi [1300 MPa]) and the elastic modulus of the strand is assumed to be 28,500 ksi (197 GPa), the expression for transfer length reduces to:

$$L_{tr} = 300\Delta \qquad (2)$$

For the production members measured at both precasting plants, the transfer length was estimated using Eq. (2).

Figure 21 shows the implied transfer lengths for the production members evaluated at plant A. From this figure, it is clear that the same trend exists whereby transfer lengths become increasingly longer for strands that are cast nearer to the top surface. In fact, the strands within the top 3 in. (75 mm) consistently had implied transfer lengths more than twice the ACI assumed value of $50d_b$ used for shear calculations.

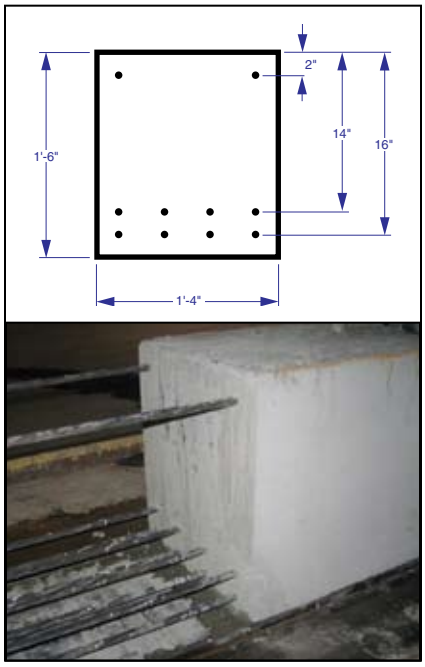

Fig. 18. Plant A 18-in.-deep rectangular beam. Note: " = inch; ' = foot. 1 in. = 25.4 mm; 1 ft = 0.3048 m.

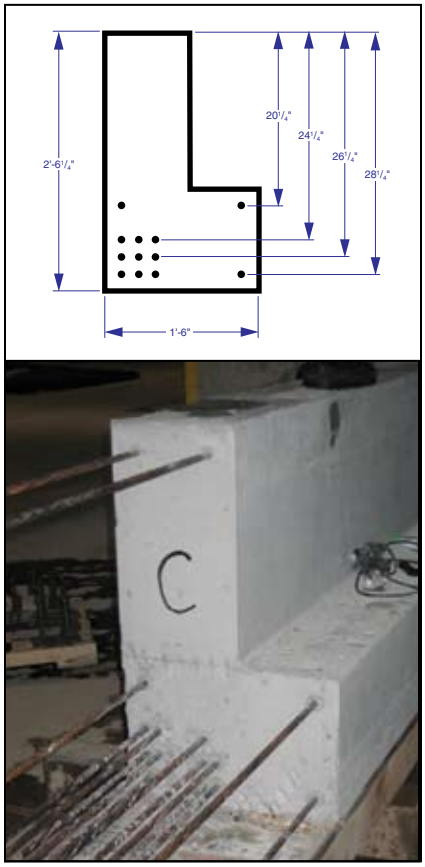

Fig. 19. Plant A 30 ¼-in.-deep L-beam. Note: " = inch; ' = foot. 1 in. = 25.4 mm; 1 ft = 0.3048 m

Fig. 20. Plant A 4-in.-thick panel. Note: 1 in. = 25.4 mm.

Table 7. Concrete Properties for Specimens Measured at Plant A

Member Type	Date of De-tensioning	Strand Size	Unit Weight, lb/ft³	Air, %	Slump Flow, in.	Release Strength, psi
Rectangular beams	4/6/06	1/2 in. special	139.2	5.0	19 1/2	4790
L-beams	4/6/06	1/2 in. special	N/A	N/A	20	3760
4-in. panels	4/7/06	1/2 in. special	139.5	4.5	19	3815
6-in. panels	4/7/06	1/2 in. special	136.4	5.0	19 1/2	4365

Note: N/A = not applicable. 1 in. = 25.4 mm; 1 psi = 6.894 kPa; 1 lb/ft³ = 16.01 kg/m³.

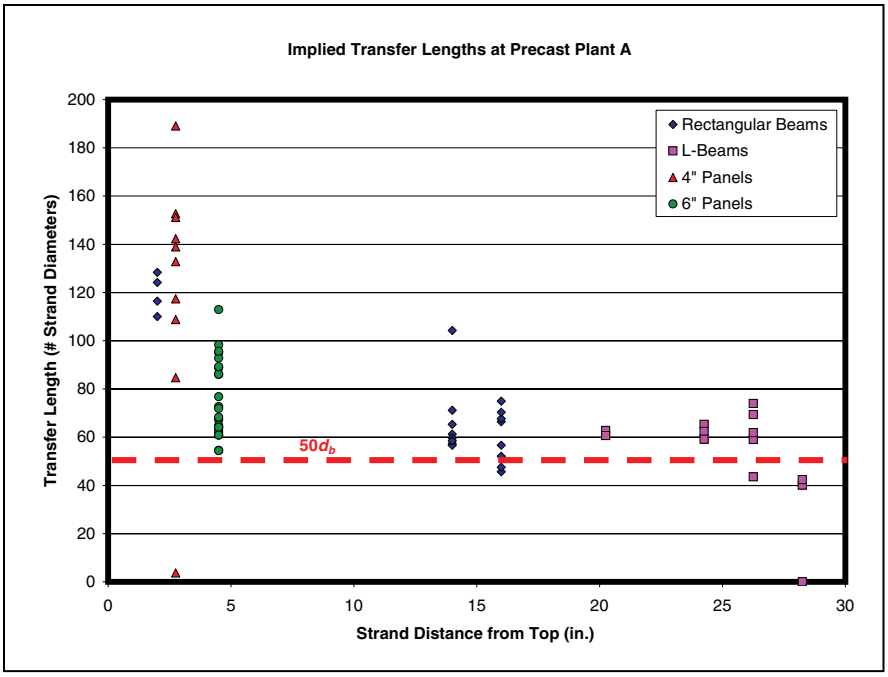

Fig. 21. Implied transfer lengths for end-slip measurements at plant A. Note: " = inch. 1 in. = 25.4 mm.

Similar measurements were also conducted at a different precasting plant (plant B) in July 2006. At plant B, several different member types were evaluated, including sandwich and solid panels, as well as deep L-beams. **Table 8** shows the specimen size, mixture proportions, and strand size for each specimen type.

As was the case with plant A, strand samples were collected at the time of the plant measurements and LBPTs were later conducted. However, in this case, the LBPTs revealed that the 9/16-in.-diameter (14 mm) strand used in the L-beams had a significantly lower bond capacity than did the other strands used at plant B. In fact, this strand failed to meet bond stress requirements equivalent to the ones recommended by Logan. What is particularly noteworthy about this finding is that the strand reel labels from both the 9/16-in.-diameter strand and the ½-in.-diameter (13 mm) strand indicated that both reels were produced by the same manufacturer.

Figure 22 shows the normalized results from LBPTs conducted on the three strands of different diameters collected at plant B during the trip to measure end-slip values. In this chart, a value greater than one means that the average of six LBPTs met the equivalent bond stress values recommended by Logan. These equivalent bond stress values were determined based on the recommended pullout loads of 16 kip (kN) for first-observed movement and 36 kip (kN) minimum ultimate pullout load for ½-in.-diameter (13 mm) strand. The 9/16 in. (14 mm) strand failed to meet both the first movement and ultimate pullout requirements.

Figure 23 shows the implied transfer lengths from measurements at plant B plotted with respect to the strand distance from the top (as-cast) surface. This figure illustrates the same overall trend of increasing transfer lengths near the top surface. However, the implied transfer lengths for the L-beams containing the 9/16 in. (14 mm) strand are extremely long (averaging 164d_b).

(continued on page 88)

ESTIMATING TRANSFER LENGTH FROM STRAND END-SLIP VALUES

Measurements of strand end slip were used to estimate the transfer length of the specimens presented in this paper.[4,18,19,20] The reason for using end-slip measurements in lieu of measuring surface displacements via gauge points mounted on the concrete's surface was to ensure de-tensioning times consistent with daily practice at PCI Producer Member plants, often as early as nine to ten hours after casting.

End-slip values were obtained by measuring the distance that the strand slipped into the specimens at the ends. Prior to de-tensioning, a small notch was made in the strand with a diamond wheel at a distance approximately 1 in. (25 mm) from the specimen end.

The distance between the mark on the strand and the panel end was measured using a digital scale having a precision of 0.001 in. (0.025 mm). This value was used as the baseline for measurements taken after de-tensioning to determine the amount of end slip. Subsequent measurements were taken up to the time of testing of each specimen. The strand end slip was then determined as the difference between final and initial measurements less the calculated elastic shortening occurring between the notch and beam end. Following are the equations used to determine the implied transfer-length values from the end-slip measurement data:

$$\Delta = \int_o^{L_{tr}} \frac{P(x)}{AE_{ps}}dx = \int_o^{L_{tr}} \frac{P(x)/A}{E_{ps}}dx = \int_o^{L_{tr}} \frac{f(x)}{E_{ps}}dx$$

where

Δ = end slip (in.)
= measured distance between mark on strand and beam end minus elastic shortening between these points

L_{tr} = transfer length (in.)

$P(x)$ = prestress force in strand (kip), varying throughout transfer length

A = cross-sectional area of strand (in.^{2})

E_{ps} = elastic modulus of strand (ksi)

$f(x)$ = stress in prestressing strand (ksi), varying throughout transfer length

Assuming straight-line variation of the strand stress at de-tensioning from zero at the member end to full initial prestress f_{si} at the end of the transfer length.

$$\Delta = \frac{f_{si}L_{tr}}{2E_{ps}}$$

Thus

$$L_{tr} = \frac{2\Delta E_{ps}}{f_{si}}$$

For the 10 in. × 15 in. (255 mm × 380 mm) specimens, initial losses were estimated to be 2.5%, with a corresponding f_{si} of 197.4 ksi (1361 MPa). The elastic modulus of the strand was reported to be 29,000 ksi (200 GPa), and the expression in Fig. 3 reduces to:

$$L_{tr} = 293.8\Delta$$

This expression is very close to the best-fit relationship presented by Russell and Burns[4] in their September–October 1996 *PCI Journal* article ($L_{tr} = 294.9\Delta$) and slightly less than the relationship used by Logan[18] ($L_{tr} = 308\Delta$). All prestress losses, and the corresponding values of f_{si} and f_{se}, noted in this paper were estimated using the procedure in the *PCI Design Handbook*.[21]

De-tensioning of the strand was achieved by flame cutting with a torch. The estimated values for transfer length were then compared with the ACI[2] assumed values of $50d_b$ (25 in. or 635 mm) (used for checking shear provisions), and the quantity $(f_{se}/3)d_b$ used for calculating the available strand stress in partially developed members. For the 10 in. × 15 in. (255 mm × 380 mm) specimens in this test program, f_{se} was estimated to be 182.2 ksi (1256 MPa), so the term $(f_{se}/3)d_b$ becomes 30.4 in. (772 mm). A similar approach was also used to estimate the strand transfer length in the 8-in.-wide × 6-in.-deep (205 mm × 150 mm) specimens.

Table 8. Concrete Properties for Specimens Measured at Plant B

Member Type	Date of De-tensioning	Strand Size, in.	Unit Weight, lb/ft^3	Air, %	Slump, in.
7-in.-thick sandwich panels	7/10/06	3/8	144.6	6.0	9 1/2
8-in.-thick solid panels	7/11/06	1/2	146.8	4.8	8
7-in.-thick solid panels	7/11/06	3/8	146.8	4.8	7 1/2
8-in.-thick solid spandrels	7/11/06	1/2	146.8	4.8	7 1/2
32-in.-deep L-beams	7/11/06	9/16	147.8	4.0	8 3/4

Note: 1 in. = 25.4 mm; 1 lb/ft^3 = 16.01 kg/m^3.

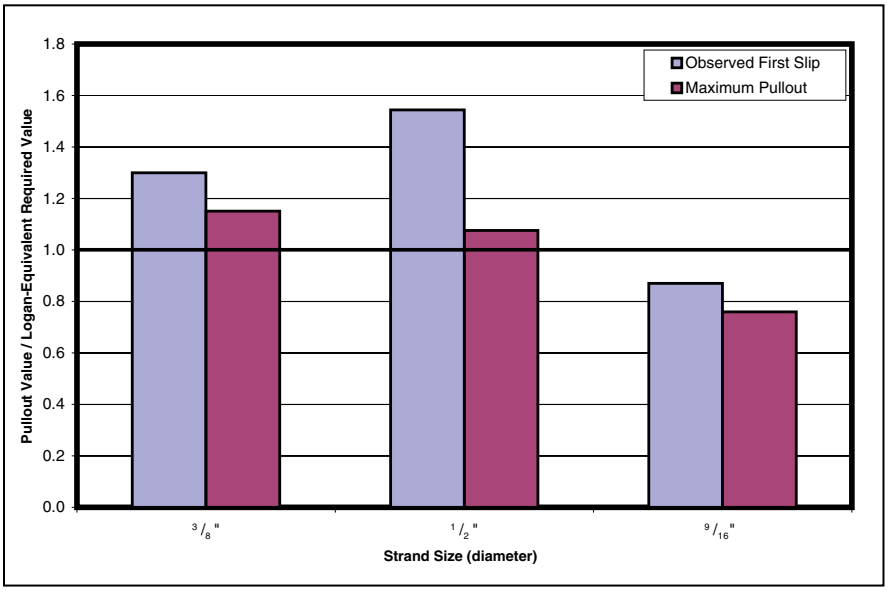

Fig. 22. Normalized large block pullout test results from plant B strands. Note: " = inch. 1 in. = 25.4 mm.

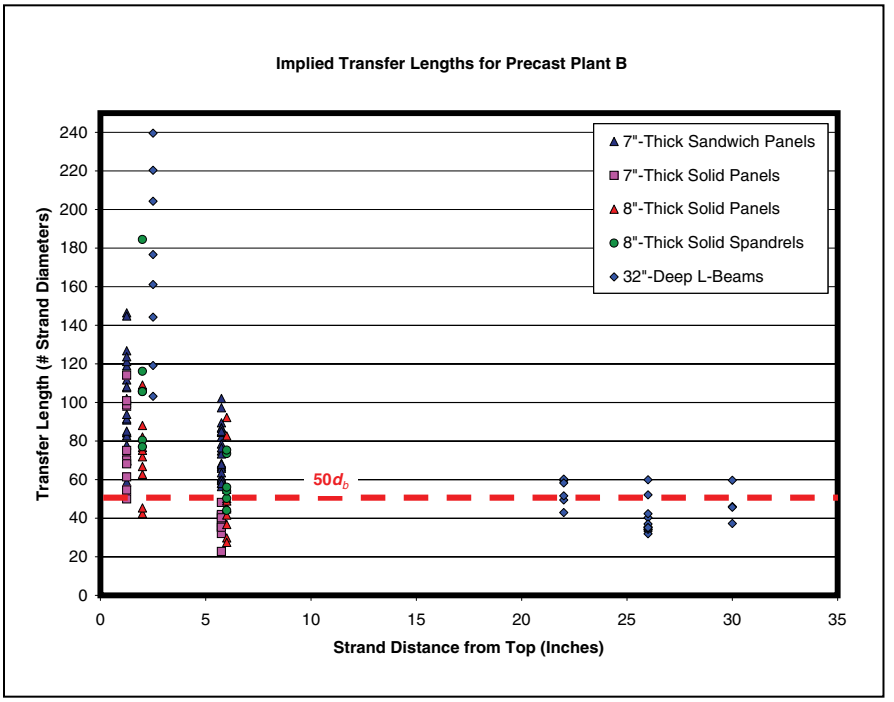

Fig. 23. Implied transfer lengths for end-slip measurements at plant B. Note: " = inch. 1 in. = 25.4 mm.

(continued from page 86)

END-SLIP MEASUREMENTS AND LOAD TESTS OF 4-IN.-THICK PANELS

Because of the unusually high end slips and implied transfer lengths that were found to be prevalent near the tops of members at several PCI Producer plants, additional tests were conducted. The objective of these tests was to determine whether the large measured end slips corresponded to a significant loss of prestress force in top-cast strands near the member ends and, if so, to determine the effect on actual load-carrying capacity. Therefore, tests were conducted on 4-in.-thick (100 mm) pretensioned panels with varying embedment lengths using both a flowable concrete and a lower-slump concrete having the same sand-aggregate ratios and water–cementitious materials ratios.

The panel specimens in this test series were 24 in. wide × 4 in. thick (600 mm × 100 mm) and contained two ½ in. special-diameter (13 mm) strands centered at a depth of 2 ½ in. (64 mm) from the top surface (**Fig. 24**). Each of these specimens had a different overall length and a crack initiator at midlength. Different panel lengths were used to determine the prestress force sustained in each length and to then compare the corresponding results with the design values assumed for partially developed strand. The crack initiator was a 1½ in. × 1½ in. × ¼ in. (38 mm × 38 mm × 6 mm) steel angle that was 24 in. (600 mm) long.

In addition to the crack former, short pieces of plastic tubing were placed around the strand at midlength (crack former location) of each panel. This

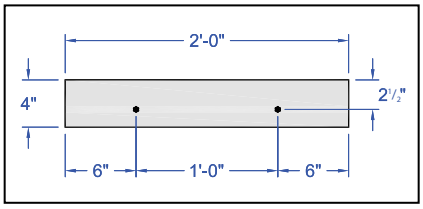

Fig. 24. Cross-section of 4-in.-thick test panels. Note: " = inch; ' = foot. 1 in. = 25.4 mm; 1 ft = 0.3048 m.

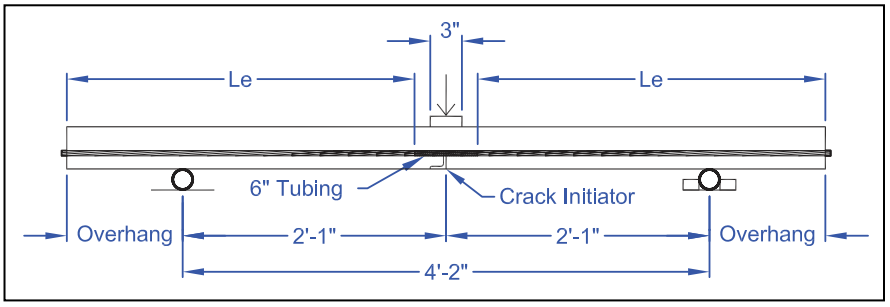

Fig. 25. Loading configuration for 4-in.-thick panel. Note: " = inch; ' = foot. 1 in. = 25.4 mm; 1 ft = 0.3048 m.

Table 9. 4-in.-Thick Specimen Designations

Specimen Designation	Embedment Length, in.	Significance
Le30	30	Slightly larger than the transfer length assumed in bilinear stress curve $(f_{se}/3)d_b$ of 29.4 in.
Le45	45	Approximately 1.5 times the quantity $(f_{se}/3)d_b$
Le60	60	Approximately 2.0 times the quantity $(f_{se}/3)d_b$

Note: 1 in. = 25.4 mm

tubing extended 3 in. (75 mm) on each side of the crack former and was used to accentuate the crack-opening point during load testing to better estimate the cracking load and, hence, to determine the remaining prestress force in each panel.

The transfer length was evaluated by doing the following:

- Measuring end slip of the strand, and
- Repeatedly loading the panels past the cracking point and determining the load required to open a crack at the midlength of the panel.

The evaluation of development length consisted of monotonically loading the panels to failure and comparing the maximum achieved moments with the ACI nominal moment capacities for the partially developed sections. Figure 24 shows the cross section of each specimen. **Figure 25** depicts the specimen geometry and the loading setup for the specimens with varying lengths.

Each test specimen had a different overall length and corresponding unique strand embedment length L_e. **Table 9** lists the specimen designations and corresponding embedment lengths along with the significance of each length tested.

Table 10 compares the mixture proportions of both the conventional concrete (batched on June 29, 2006) and the flowable concrete (batched on April 6, 2006). Internal vibration was used during the casting of the conventional and the flowable concrete specimens. **Table 11** shows the properties of both mixtures. A design compressive strength of 6000 psi (41 MPa) was assumed for both mixtures when performing all calculations. Strand samples were collected at the time of casting each specimen set, and LBPTs revealed that the strand used in both

Table 10. Concrete Mix Proportions for 4-in.-Thick Panel Tests

Materials	Flowable	Conventional
Cement (type 3)	700 lb	700 lb
Class C fly ash	120 lb	120 lb
Sand	1100 lb	1100 lb
Granite	1635 lb	1635 lb
Air-Entraining admixture	7.0 oz	7.0 oz
Type F HRWRA	34 oz	28 oz
Type A, B, D water reducer & retarder	0 oz	24 oz
Water	290 lb	290 lb
Water–cementitious materials ratio	0.35	0.35

Note: HRWRA = high-range water-reducing admixture. 1 in. = 25.4 mm; 1 lb = 0.453 kg; 1 oz = 29.6 mL.

Table 11. Concrete Properties for 4-in.-Thick Panel Tests

Property	Flowable	Conventional
Spread or slump flow, in.	$19^1/_2$	$7^3/_8$
Air content, %	5.0%	5.5%
Concrete temperature, ˚F	77	92
Compressive strength at release, psi	4365	4440
28-day compressive strength, psi	6850	6985

Note: 1 in. = 25.4 mm; 1 psi = 6.89 kPa; ˚F = (˚F - 32)/1.8.

Fig. 26. Two linear variable displacement transducers were used to detect the opening of the midspan crack. Note: " = inch. 1 in. = 25.4 mm.

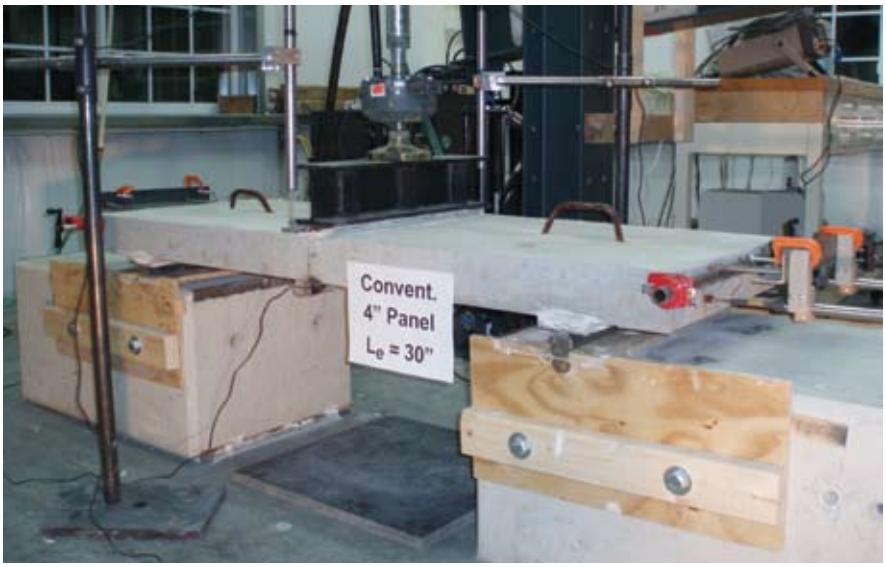

Fig. 26. Two linear variable displacement transducers were used to detect the opening of the midspan crack. Note: " = inch. 1 in. = 25.4 mm.

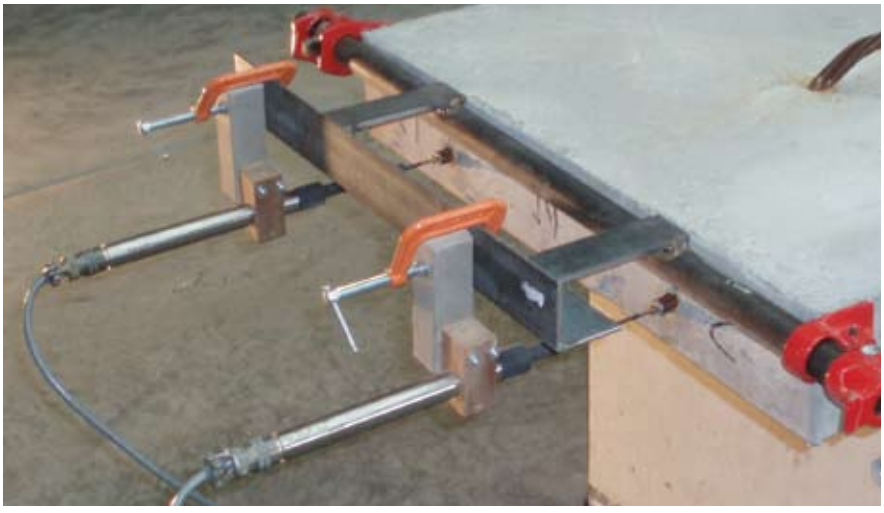

Fig. 28. Linear variable displacement transducers used to detect additional strand slip at each end of the specimen.

the flowable and conventional panels met the minimum requirements recommended by Logan.

In addition to using strand end-slip readings to estimate transfer lengths in the panels, the prestress force in each specimen was also determined from the member response during load tests. Each specimen was loaded in center-point bending according to the specimen test arrangements shown in Fig. 25. Each specimen was initially loaded until a crack was observed at the location of the crack former. Next, the specimen was unloaded and then reloaded to determine the value at which the crack would reopen. This process was repeated several times for each specimen.

Precise visual determination of the crack-opening load was not possible due to the surface anomalies associated with the presence of the crack former. Instead, the crack-opening load was determined from linear variable displacement transducers (LVDTs) that spanned the crack initiator on the bottom face of each panel (**Fig. 26**) and also by examining the load-deflection response obtained using LVDTs at midspan (**Fig. 27**). This is similar to the technique used by Larson, Peterman, and Rasheed.[24] There were two midspan deflection LVDTs, two crack-opening LVDTs, and four strand end-slip LVDTs (one per strand) that were used to determine any additional slip of the strands that occurred during the loading process (**Fig. 28**).

Table 12. Crack Opening Loads, Moments, and Calculated Prestress

	Specimen	Crack-Opening Load, lb	$M_{applied}$ at Crack Initiator, lb-in.	M_{self} at Crack Initiator, lb-in.	$M_{cr\text{-}0}$ at Crack Initiator, lb-in.	Calculated Prestress Force, lb	Calculated Prestress,* ksi
Flowable	Le30	3500	200	2200	45,400	38,900	116
	Le45	5300	65,000	380	65,380	56,000	168
	Le60	5700	69,800	-3220	66,580	57,100	171
Conventional	Le30	4000	49,200	2200	51,400	44,100	132
	Le45	5500	67,400	380	67,780	58,100	174
	Le60	5800	71,000	-3220	67,780	58,100	174

Note: 1 lb = 0.453 kg; 1 lb-in. = 0.112 N-m; 1 ksi = 6.894 MPa.

* f_{se} was estimated to be 168.8 ksi for the 4-in.-thick panels using the *PCI Design Handbook* procedure.

The reason for initially loading the panel past the crack-opening load was to eliminate any tension carried by the concrete at the location of the crack initiator. After identifying the crack-opening load for each specimen, the moment required to reopen the crack at the crack-initiator location $M_{cr\text{-}0}$ was calculated from static equilibrium. Then, the internal prestress force P was determined from the following expression.

$$-\frac{P}{A}-\frac{Pe}{S}+\frac{M_{cr-0}}{S}=0$$

where

e = strand eccentricity
= 0.5 in. (13 mm)

$M_{cr\text{-}0}$ = total moment (due to self-weight and applied load) when the crack reopens at the crack-initiator location (zero-concrete tension)

A = cross-sectional area of the 4-in.-thick (100 mm) specimen
= 96 in.^{2} (62,000 mm^2)

S = elastic section modulus
= 64 in.^{3} (1.05 × 10^6 mm^3)

This internal prestress force P and corresponding strand stress f_s were then compared with the internal force determined for the other specimens with varying embedment lengths and with the estimated effective prestress stress f_{se} of 168.8 ksi (1164 MPa). Because each of the specimens had an embedment length greater than or equal to the calculated transfer length of 29.4 in. (747 mm), the theoretical prestress force in each member should have been identical. Note, f_s is equal to $P/(2 \times 0.167$ in$^2)$ for the panels with two $^1/_2$ in. special-diameter (13 mm) strands. The self-weight of the 4 in. × 24 in. (100 mm × 600 mm) panels was calculated to be 7.85 lb/in. (94.25 lb/ft [140 kg/m]). Since the determination of the cracking load is somewhat subjective, this load was reported only to the nearest 100 lb (45 kg).

Table 12 lists the crack-opening loads, corresponding moments, and the calculated prestress force in each of the six panel specimens (three made with conventional concrete and three made with the flowable mixture). The load test results indicate that there was indeed a significant loss of prestress force in both specimens with an embedment length equal to 30 in. (760 mm), which was just longer than the assumed value for transfer length $(f_{se}/3)d_b$. The implied remaining stress in the strands was 116 ksi (800 MPa) for the flowable concrete and 132 ksi (910 MPa) for the conventional concrete. According to the design assumptions, the internal prestress should have been greater than or equal to the effective prestress stress of 168.8 ksi (1164 MPa).

The values of prestress stress in Table 12 were then used to estimate the corresponding transfer length by assuming a linear variation on stress until full prestress would be effective. Full prestress was assumed to be the remaining prestress calculated for the corresponding members with a 60 in. (1520 mm) embedment length.

Table 13 shows the transfer lengths estimated from both load testing and strand end-slip measurements. The values for transfer lengths calculated from both of these methods are in excellent agreement. Thus, it seems that the use of strand end-slip measurements does provide a good estimate of the member transfer lengths. This table also indicates that in each case the transfer lengths were considerably longer than the values of $(f_{se}/3)d_b$ (29.4 in. [747 mm]) and $50d_b$ (26.1 in. [663 mm]).

Table 14 lists the average implied transfer lengths for the three panels made with flowable concrete (48 in. [1220 mm]) and the three made with conventional concrete (37 in. [940 mm]). These were estimated from the average of 12 end-slip measurements (three panels each with four strand ends). These values are both greater than the assumed values as shown in the table. In addition, the panels made with flowable concrete had average transfer lengths that were 30% longer than those for panels made with conventional concrete.

After the crack-opening load was

Table 13. Implied Prestress Stress and Transfer Lengths for Specimens with Flowable Concrete

	Specimen	Calculated Prestress, ksi	L_{tr} from Load Tests, in.	L_{tr} from Strand End-Slip Measurements, in.
Flowable	Le30	119.5	45	>46*
	Le45	167.8	46	45
	Le60	171.0	Assumed <60	54
Conventional	Le30	132.0	40	>38*
	Le45	174.0	≤45	37
	Le60	171.0	Assumed <60	33

*Because the use of Eq. (2) resulted in an implied transfer length longer than the embedment length, this value was estimated by compatibility of deformations with the assumption of a linear stress variation throughout the transfer length.
Note: f_{se} was calculated to be 168.8 ksi for the 4-in.-thick panels. 1 in. = 25.4 mm; 1 ksi = 6.894 MPa.

Table 14. Comparison of Average Transfer Lengths with Code Expressions

Mix	Average L_{tr} at Testing, in.	Compared with $50d_b$	Compared with $(f_{se}/3)d_b$
Flowable	48	1.84	1.64
Conventional	37	1.41	1.25

Note: There was a 30% increase in average transfer lengths when the concrete fluidity was increased. 1 in. = 25.4 mm.

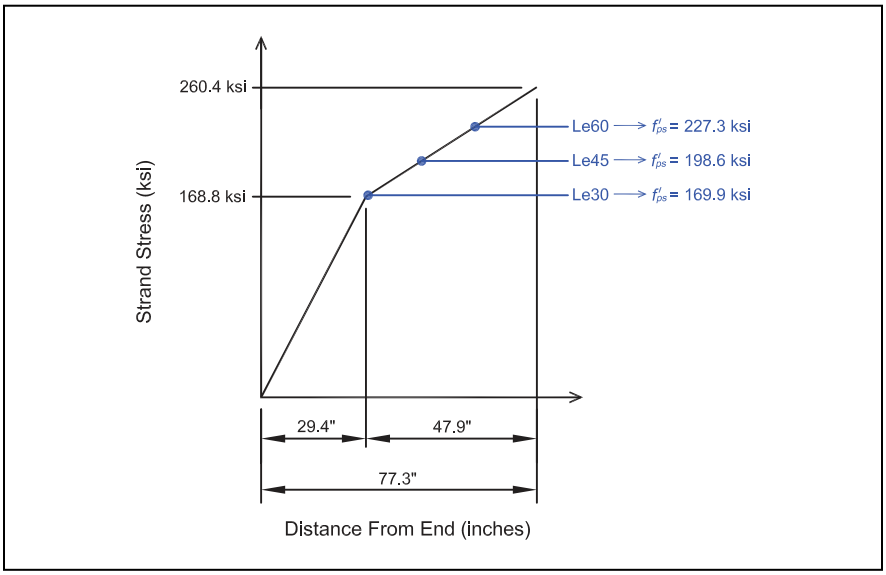

Fig. 29. Calculated prestress stress at nominal capacity for the partially developed strands. Note: " = inch. 1 in. = 25.4 mm; 1 ksi = 6.895 Pa.

Table 15. Maximum Applied Load and Corresponding Ultimate Moment Capacity

	Specimen	Maximum Applied Load, lb	Ultimate Applied Moment, lb-in.	M_u, lb-ft
Flowable	Le30	8090	100,970	8410
	Le45	9940	121,640	10,140
	Le60	11,890	141,620	11,800
Conventional	Le30	11,650	144,140	12,010
	Le45	14,890	181,680	15,140
	Le60	16,380	196,150	16,380

Note: 1 lb = 4.45 kN; 1 lb-in. = 0.112 N-m.

determined for each panel, the panels were then loaded to failure to determine their ultimate moment-carrying capacity. **Table 15** shows the maximum applied loads and corresponding ultimate moments for each specimen.

Because these specimens had embedment lengths less than the calculated development lengths of the strand (77.3 in. [1960 mm]), it was expected that each of the specimens would fail in bond. Indeed, each of the three specimens made with flowable concrete experienced bond failures. However, only specimen Le30 with the conventional concrete experienced a true bond failure. Specimen Le45 failed in a combined manner in which one strand failed by strand rupture and the other strand experienced more than $^1/_2$ in. (13 mm) of end slip. Specimen Le60 failed in flexure when both prestressing strands ruptured in tension.

The ultimate moments in Table 15 were then compared with the theoretical capacities for the panels to determine whether the sections met the current ACI design assumptions for nominal moment capacity based on the design strength of 6000 psi (42 MPa). The 28-day strength of the flowable concrete was 6850 psi (48 MPa), while the 28-day strength of the conventional concrete was 6985 psi (49 MPa).

Because each specimen had a different embedment length, the stress in the strand at nominal capacity was calculated from the bilinear strand develop-

Table 16. Comparison of Ultimate Moments with Calculated Nominal Moment Capacities

	Specimen	f'_{ps}, ksi	Analysis Assuming ε_c = 0.003		Analysis Using Martin-Korkosz Method	
			M_n, lb-ft	M_u/M_n	M_n, lb-ft	M_u/M_n
Flowable	Le30	169.9	10,730	0.784*	8040	1.05
	Le45	198.6	12,320	0.823*	11,000	0.921*
	Le60	227.3	13,850	0.852*	13,080	0.903*
Conventional	Le30	169.9	10,730	1.12	8040	1.49
	Le45	198.6	12,320	1.23	11,000	1.38
	Le60	227.3	13,850	1.18	13,080	1.25

* Values indicate that the specimens failed below the nominal moment capacity. Note: 1 lb-ft = 1.356 N-m; 1 ksi = 6.894 MPa.

ment curve presented in section 12.9 of ACI 318. The expression for f'_{ps}, as presented in PCI's *Manual for the Design of Hollow Core Slabs*,[25] is the following:

$$f'_{ps} = f_{se} + \frac{\left(x - L_{tr}\right)}{L_f}\left(f_{ps} - f_{se}\right)$$

where

f_{ps} = stress in prestressed strand at nominal strength of the fully developed section (calculated to be 260.4 ksi [1800 MPa] by strain compatibility for the 4-in.-thick [100 mm] panels, assuming f'_c = 6000 psi [41 MPa])

f_{se} = effective stress in prestressed strand after all losses (estimated as 168.8 ksi [1164 MPa] for the section)

x = the strand embedment length (in.)

L_{tr} = the transfer length (in.), predicted (by ACI 318) as

$$L_{tr} = \frac{\left(f_{se}\right)}{3} d_b = 29.4 \text{ in.}$$

(750 mm) for the section

L_f = the flexural bond length (in.)
= $(f_{ps} - f_{se})d_b$
= 47.9 in. (1220 mm) for the section

Figure 29 shows the bilinear stress curve for the 4-in.-thick (100 mm) specimens along with the calculated values of f'_{ps} for each of the four test specimens. This reduced prestress force was then used to calculate the nominal moment capacity of each specimen using two different procedures. The first procedure is the so-called traditional analysis in which the concrete is assumed to reach a maximum compressive strain of 0.003 at incipient failure. The author learned through discussions with several design engineers at the precasting plants he visited that the assumption of a compressive strain of 0.003 is often used when calculating the nominal moment capacity of partially developed sections.

The second procedure used was the one recommended by Martin and Korkosz[26] and later referenced in the *Manual for the Design of Hollow Core Slabs*. Using this iterative analysis procedure, the concrete strain and stress distribution is assumed to remain linear, and a strain compatibility analysis is performed in order to satisfy equilibrium of internal forces.

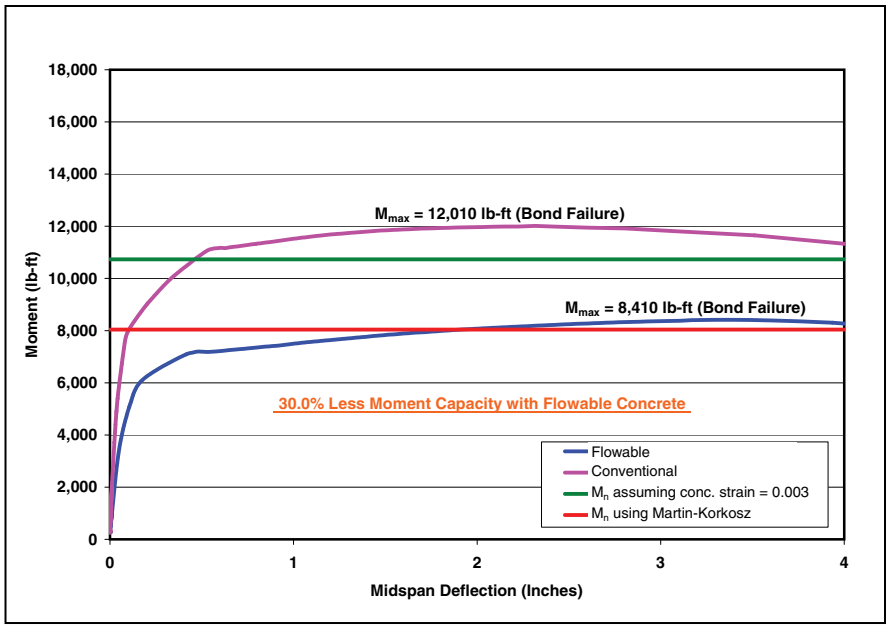

Fig. 30. Moment versus deflection graph of specimen Le30. Note: 1 in. = 25.4 mm; 1 lb-ft = 1.356 N-m.

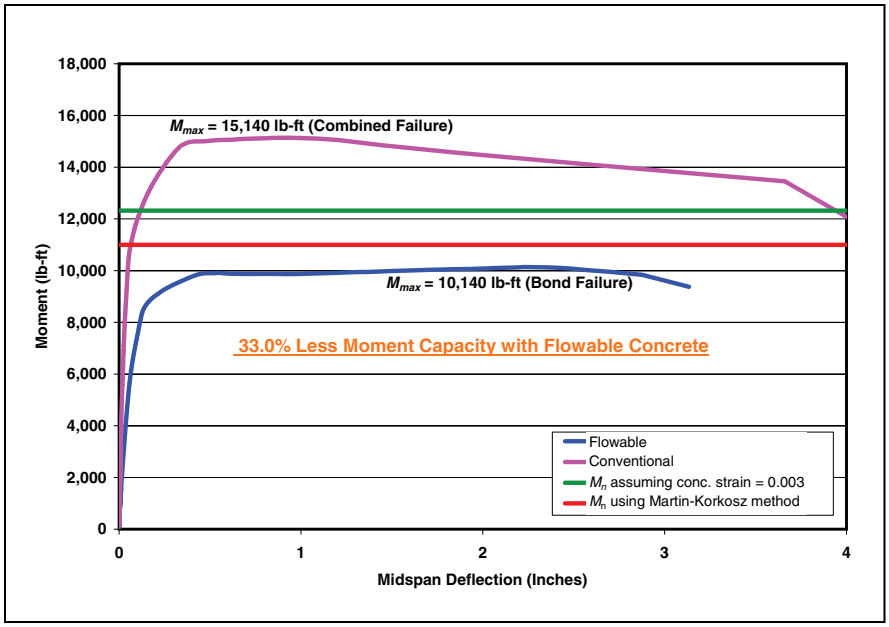

Fig. 31. Moment versus deflection graph of specimen Le45. Note: 1 in. = 25.4 mm; 1 lb-ft = 1.356 N-m.

Table 16 indicates that the maximum moment attained in all three flowable concrete specimens was less than the nominal moment capacities based on both of the traditional analyses, assuming a compressive strain of 0.003. The deficiency varied from 14.8% to 22.6% using the traditional analysis. The maximum moments attained in specimens Le45 and Le60 were also less than the nominal capacity calculated using the Martin-Korkosz method. The deficiencies were 7.9% and 9.7%, respectively, for these specimens when assuming linear-elastic concrete behavior.

All three specimens with conventional concrete exceeded the nominal moment capacities computed using both the traditional and Martin-Korkosz methods. However, the use of a flowable concrete with the same sand–

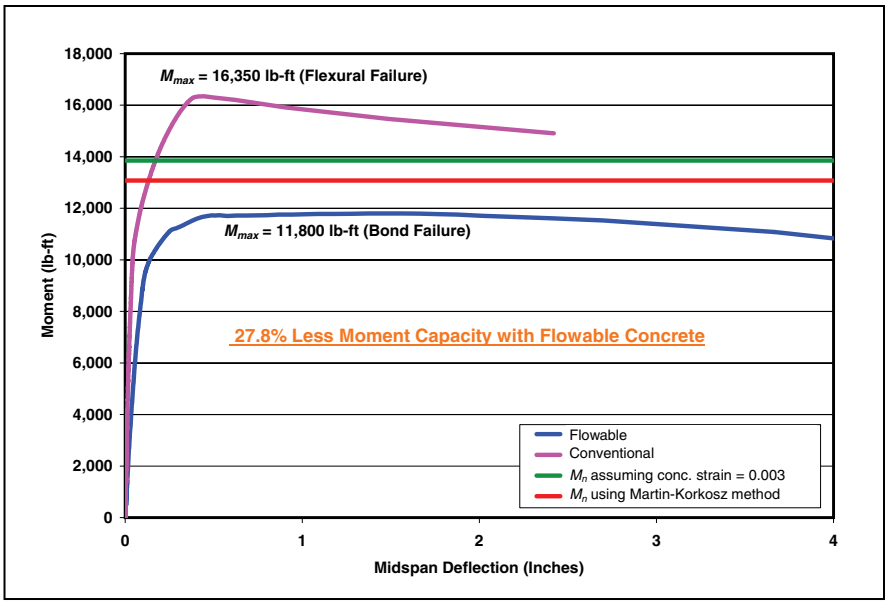

Fig. 32. Moment versus deflection graph of specimen Le60. Note: 1 in. = 25.4 mm; 1 lb-ft = 1.356 N-m.

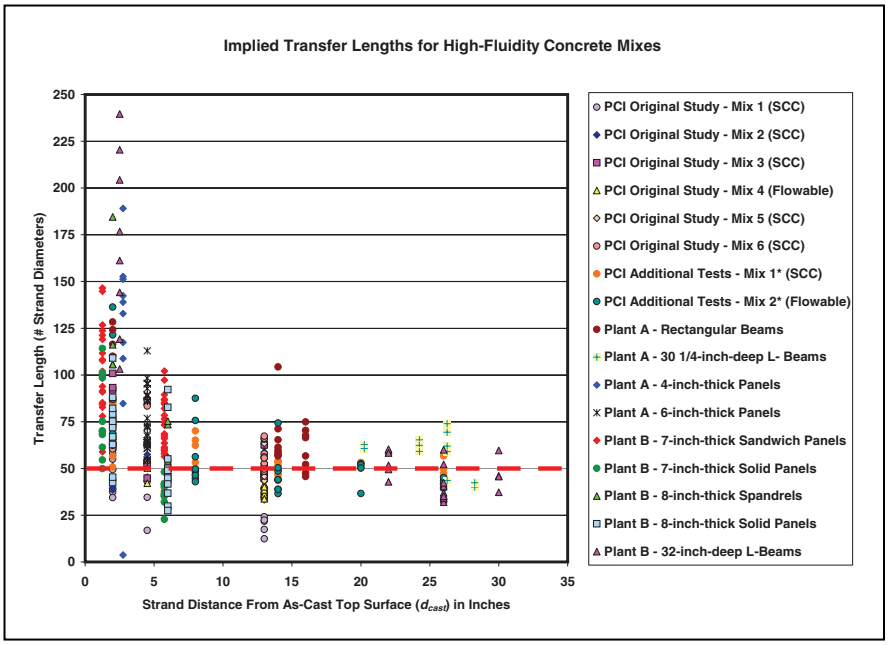

Fig. 33. Implied transfer lengths based on 372 strand end-slip measurements. Note: SCC = self-consolidating concrete. 1 in. = 25.4 mm.

aggregate ratio and water–cementitious materials ratio seemingly resulted in a reduction in both prestress force and ultimate load-carrying capacity. On average, the specimens using a flowable concrete had a 30% lower moment capacity than those using conventional concrete. **Figures 30** through **32** show the moment versus deflection graphs for specimens Le30, Le45, and Le60, respectively. In these figures, the green horizontal line represents the nominal moment capacity calculated by assuming a concrete compressive strain of 0.003. The red horizontal line is the nominal moment capacity calculated using the Martin-Korkosz method.

REDUCING THE DATA INTO DESIGN APPROXIMATIONS

Figure 33 shows the transfer lengths implied by 372 different strand end-slip measurements made on specimens made with concrete that had a high fluidity. All of the measurements were taken during the period beginning January 2005 and ending July 2006. This figure includes all of the end-slip measurements from the original PCI SCC study, the normalweight, high-fluidity mixtures from the additional PCI testing series to de-couple the top and bottom casting distances, and the strand end-slip measurements made on production members at plants A and B. **Figure 34** plots the average data points from the same set of readings.

The author acknowledges that there exists an inconsistency in ages for the implied transfer lengths in Fig. 33 and 34. For the original PCI study, the strand end-slip measurements were made at 21 days because the specimens were load tested between 25 and 38 days. For the additional series to de-couple the top and bottom casting distances, the end-slip measurements were made after 90 days. In addition, the measurements made at precasting plants A and B were made during the first two days after de-tensioning. Therefore, it is likely that these latter end-slip measurements would have increased with time, making the average implied transfer lengths somewhat larger than the values shown in the figures.

From these two figures, it is clear that the transfer lengths can be quite long for strands near the top surface, especially when compared with the current ACI design assumption of $50d_b$ (see "Code Provisions for Bond in Pretensioned Members" on p. 76). In addition, there is significant scatter in the data. Another observation from these figures is that there are no data points between the depths of 8 in. and 13 in. (200 mm and 325 mm) because none of the products measured by the author had strand depths within that range. This gap also appears to be a place of transition between the higher transfer lengths of strands cast near the top surface and lower transfer lengths associated with strands located further down in the members. Therefore, the data were separated into two sets, and best-fit lines were drawn through each group. Prior to doing this, however, the data corresponding to the L-beams from plant B (with the strand that did not meet the LBPT requirements) was

removed from the data set so that all of the data would be representative of good-bonding strand. **Figure 35** shows these two data sets.

The trend line for strands with depths greater than or equal to 13 in. (325 mm) was nearly horizontal, so a best-fit horizontal line was placed through the data. This best-fit horizontal line has a constant transfer length of $50.2d_b$. Therefore, the assumption that transfer length L_t is equal to $50d_b$ is a realistic average number for strands cast deeper in concrete members.

The trend line for the strand transfer lengths near the top surface yielded a best-fit line with the equation $L_t = 93.1 - 5.32d_{cast}$, where d_{cast} is defined as the strand depth from the top surface of concrete placement. Setting L_t equal to 50 and solving for d_{cast} yields 8.081. Therefore, the transition point between the two best-fit lines is essentially at a depth d_{cast} of 8 in. (200 mm). The y-intercept for this equation is 93.1, so an assumption of $90d_b$ for the uppermost value seems reasonable.

Figure 36 shows the simplified bilinear approximation of the average data. Because there is always a minimum amount of top cover over a strand, a theoretical average value less than $90d_b$ would always apply. If a minimum as-cast strand depth d_{cast} of 2 in. (50 mm) is assumed, then the bilinear relationship would imply an average transfer length of $80d_b$ at this location. Therefore, a stepped relationship having a maximum value of $80d_b$ could also be used to reasonably represent the average transfer-length data. **Figure 37** shows one such relationship.

In Fig. 37, a top-cast strand with a depth d_{cast} of less then 4 in. (100 mm) would be assumed to have a transfer length of $80d_b$. This is the equivalent of a 1.6 multiplier on the existing assumption of $50d_b$. For a depth d_{cast} between 4 in. and 8 in. (100 mm and 200 mm), the transfer length would be $65d_b$. This is the equivalent of a 1.3 multiplier on the existing assumption of $50d_b$.

The decision to include all of the data from good-bonding strand in this analysis and not to separate out the SCCs from the high-slump/flowable mixtures was made for the following reasons. First, through the work at the six precasting plants reported herein, the author has observed that many mixtures that begin as true SCCs (slump flows greater than 23 in. [580 mm]) at the batch plant undergo significant slump loss between the time of initial batching and the end of casting, especially during hot weather. Therefore, the author has observed that such mixtures often undergo a transition between SCC and flowable mixtures during placement activities, with the latter occasionally needing vibration to complete the casting operation.

Additionally, one of the plants that selected the admixture suppliers for the initial PCI SCC study was actually producing a flowable concrete, not a true SCC. The term SCC has often been loosely used by many precasters to include mixtures that are actually flowable mixtures, with slump flows (spreads) between 18 in. and 23 in. (460 mm to 580 mm).

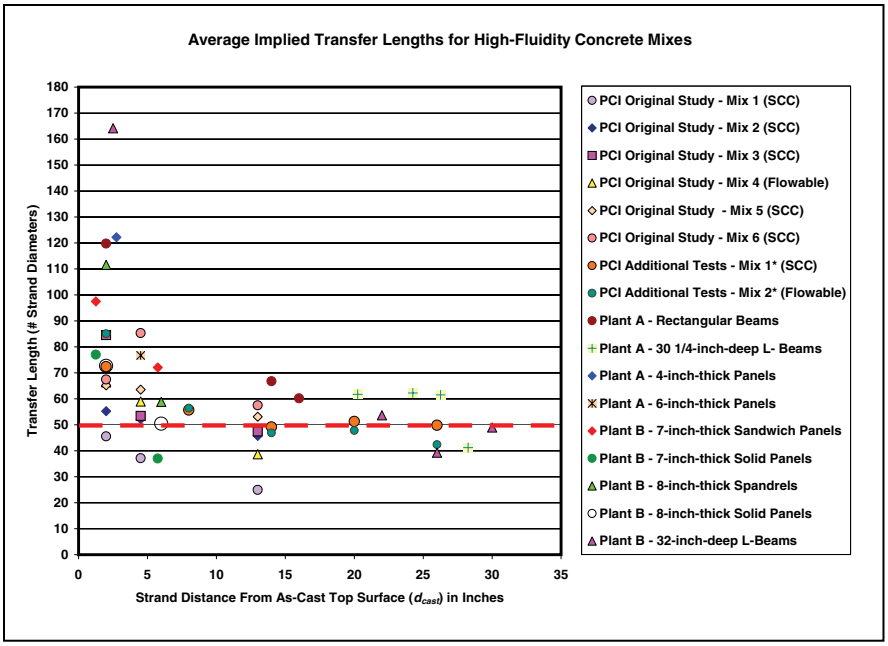

Fig. 34. Average implied transfer lengths for different member types. Note: SCC = self-consolidating concrete. 1 in. = 25.4 mm.

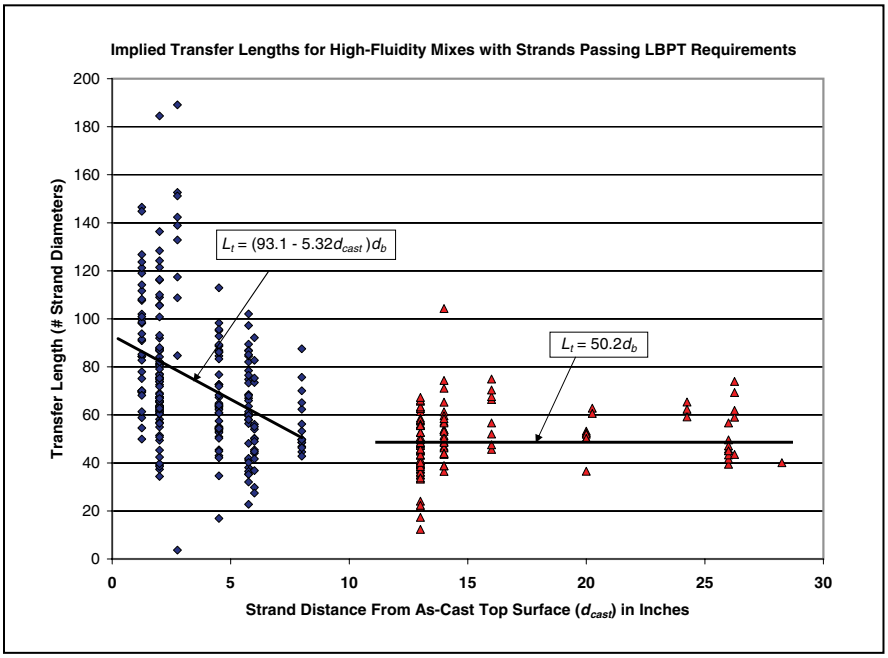

Fig. 35. Data divided into two groups with trend lines. Note: 1 in. = 25.4 mm.

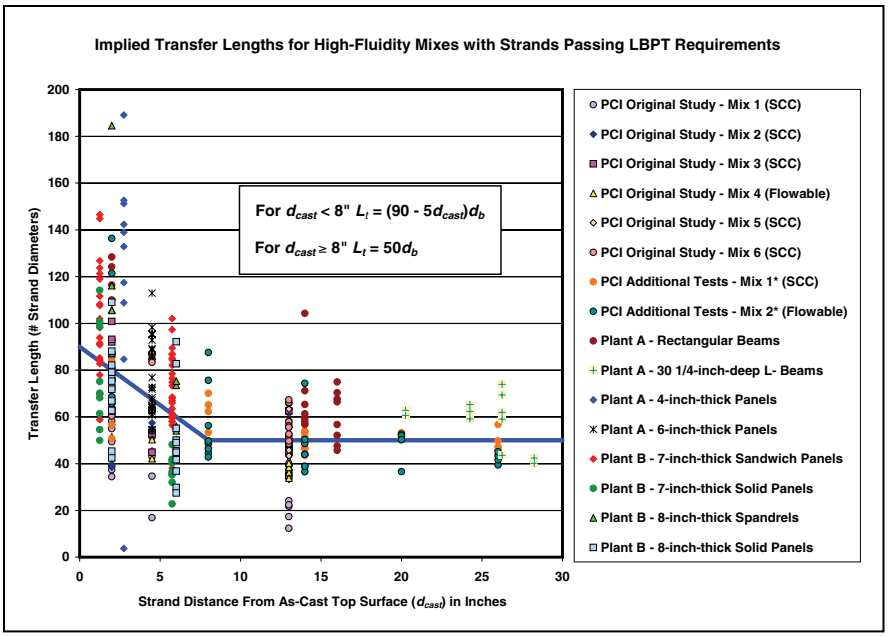

Fig. 36. Bilinear approximation of average transfer length data. Note: SCC = self-consolidating concrete. 1 in. = 25.4 mm.

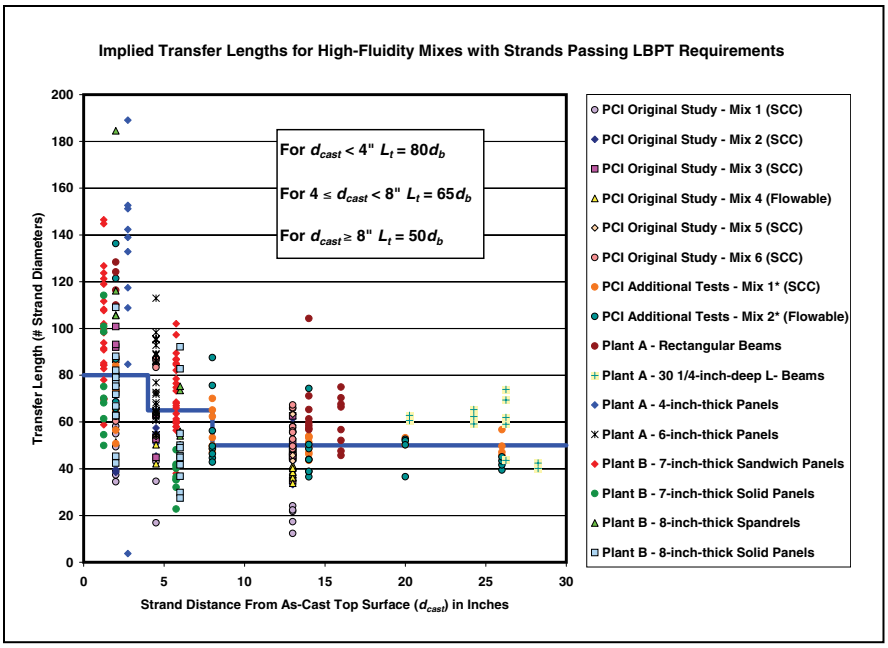

Fig. 37. Stepped approximation of average transfer-length data. Note: LBPT = large block pullout test; SCC = self-consolidating concrete; " = inch. 1 in. = 25.4 mm.

CONCLUSIONS

Based on the work described in this paper, the following conclusions may be drawn:

- All of the bottom-strand specimens, which utilized the project strand in the original test series and met the LBPT requirements stipulated by Logan, had average implied transfer lengths that were in good agreement with the ACI design assumptions. However, a beam with the identical cross section and lower-bonding strand had an average transfer length that was nearly 40% longer than the ACI design assumption of $(f_{se}/3)d_b$ and nearly 70% longer than the assumption of $50d_b$ used in shear calculations.
- Strand end-slip measurements and their implied transfer lengths revealed that the bond between strand and SCCs was a function of the as-cast position of the strand in the specimens. Strands cast near the bottoms of 15-in.-deep (380 mm) specimens had implied transfer lengths that were generally less than current ACI design assumptions. However, strands cast near the tops of similar specimens had average transfer lengths that were approximately 30% longer than the ACI-assumed value of $50d_b$, with one mixture having average values nearly 70% larger.
- Although several specimens in the original test series had implied transfer lengths that were significantly larger than the ACI assumed values, these specimens were still able to withstand their design nominal moment capacity when loaded to failure.
- Additional end-slip measurements on strands with varying distances from the bottom and top surfaces revealed that the top-strand effect is primarily a function of the depth of the strand from the top of concrete placement surface (defined as d_{cast} herein), not the amount of concrete below the strands. This finding is in agreement with the current understanding of the top-bar effect for deformed bars as presented in ACI 408R-03.[32]
- Strand end-slip measurements on standard production members at two PCI Producer Member plants exhibited a similar trend of increasing strand end slips with a reduction of strand depth from the top casting surface. The implied transfer lengths at both plants for top-cast strands were considerably larger than current design assumptions. At one of the plants, a strand that exhibited a significantly lower bond performance in LBPTs yielded average implied transfer lengths of $164d_b$ when positioned near the top (as-cast) surface.
- Tests with both conventional concrete and high-fluidity concrete indicate that when keeping the water–cementitious materi-

als ratio of a mixture constant, an increase in fluidity will result in a reduction in bond capacity. The effect becomes even more pronounced near the top (as-cast) surface. This finding is consistent with previous findings related to the top-bar effects in pretensioned piles[14] and also with the current understanding of the effect of concrete fluidity on the bond of deformed bars.[32]

- None of the rheological properties measured for the SCCs in this study (VSI, spread, J-ring, column segregation, and L-box differential) showed consistent correlation with the bonding capability or strand-depth effect of the SCCs evaluated. In the original test series, mix 2 had the highest column segregation value (0.58) yet the second-best bonding capability in the top-strand specimens.
- Load tests on 4-in.-thick (100 mm) pretensioned panels with varying embedment lengths indicated that the strand end-slip measurements were good predictors of the actual member transfer lengths. These same tests revealed that the average transfer lengths for members with a flowable concrete were, on average, 30% longer than similar panels containing a conventional concrete with a $7^3/_8$ in. (187 mm) slump. A similar percentage reduction in ultimate load-carrying capacity was also noted in all three specimens. Two of the three specimens failed in bond below the calculated ACI nominal moment capacity.

DISCUSSION

This paper summarizes the findings from strand end-slip measurements and load tests on members produced at six different PCI Producer Member precasting plants during the past two and a half years using standard production mixtures and placement techniques. As such, the data presented herein are believed to be a representative sample of current industry practice. The findings of this study indicate that, in general, the assumption of a transfer length equal to the single value of $50d_b$ or $(f_{se}/3)d_b$ is largely unconservative for members with pretensioned strands located near the top (as-cast) surface. This effect seems to be exacerbated when high-fluidity concrete is used.

The top-strand effect was determined to be primarily a function of the as-cast depth of the strand from the top surface, rather than the amount of concrete cast below the reinforcement (as implied by current code expressions for deformed top bars). The data indicate that this effect varies largely among mixtures. In addition, some mixtures may experience large differential ratios between transfer lengths for top- and bottom-cast strands and still have relatively low overall transfer lengths (such as noted for mix 1). Unfortunately, the rheological properties measured at the time of casting (slump flow, J-ring, VSI, L-box) were not found to be consistent indicators of the resulting bond performance of a mixture.

In the additional tests used to decouple the top and bottom strand distances, the bond for the lightweight mixture (mix 4* flowable) was significantly lower than the bond of the similar mixture (mix 4) in the original test program. The original test series was conducted in spring 2005, while the additional test series was conducted in summer 2006.

When comparing Table 2 with Table 5, it is obvious that mix 4* flowable (cast during warmer weather) utilized two different retarding admixtures that were not used for mix 4 in the original test series. Thus, it seems plausible, based on the findings of Wan et al.,[14] that these retarding admixtures may have contributed to the noted reduction in bond for the top-cast strands. A similar observation was also made when analyzing the original test series data, in which mix 3 had the highest top-strand effect and was the only mixture containing a retarding admixture.

If the noted top-strand effect is primarily caused by bleeding and settling, then an admixture that acts to delay the initial set would allow more time for these phenomena to occur, resulting in a more pronounced effect.[31] It is also likely, then, that there may be ways to reduce these negative consequences. For example, Khayat et al.[34] demonstrated that using a viscosity-modifying admixture (VMA) could enhance the stability of fluid concrete, thereby limiting the top-bar effect. In addition, Attiogbe et al.[35] found that highly stable SCCs incorporating VMAs can be produced to have a level of top-bar effect for deformed bars that is similar to the top-bar effect in a 4-in.- to 6-in.-slump (100 mm to 150 mm) concrete.

While there may be ways to reduce the adverse top-strand effect noted by the author, possibly through the use of VMAs or different proportioning methods, none of the precasting plants participating in the PCI research program used a VMA in its production mixture. Furthermore, the mixtures selected for evaluation in this study were proportioned with the assistance of the admixture suppliers, and the admixture suppliers selected the participating precasting plants for inclusion in this study because their procedures were believed to be the most representative of current industry practice.

The findings in this study indicate that the average transfer lengths for members cast within 2 in. (50 mm) of the top surface were, on average, more than 60% longer than the amount currently assumed by design engineers ($50d_b$). This average value was for strand that met the minimum pull-out values recommended by Logan in LBPTs. The end-slip measurements on production members (at plant B) containing strand that failed to meet the LBPT acceptance criteria yielded average implied transfer lengths ($164d_b$) that were 220% longer than the transfer length ($50d_b$) assumed by design engineers.

While this study has shown that transfer lengths of top-cast strands can be considerably longer than currently assumed design values, the actual development lengths of these strands were not found to increase in the same proportion for the specimens tested. In the original test series, all specimens were able to withstand the calculated ACI nominal moment capacity, even though the top-strand specimens cast with mix 3 had implied transfer lengths in ex-

(continued on page 99)

ORIGIN OF THE TOP-BAR MULTIPLIER IN U.S. CODES

Because the findings in this study differ significantly from the traditional understanding of the top-bar effect for prestressed strands, the author reviewed the origins of the current top-bar requirements for deformed bars. The first code appearance of a top-bar effect for reinforcement was in ACI 318-51,[27] and these provisions were heavily influenced by the experimental work of Clark.[6,7] In his work, Clark tested specimens that were 18 in. deep (450 mm) and had a single bar cast near each top and bottom surface. Clark concluded that in the top position, bars "were about two-thirds as effective in bond as in the bottom position." Hence, in ACI 318-51, the allowable bond stresses for deformed bars were limited to the following:

- $\mu = 0.07 f_c'$ for top bars
- $\mu = 0.08 f_c'$ for two-way footings (except top bars)
- $\mu = 0.10 f_c'$ for all other cases

ACI 318-51 defined top bars as horizontal bars placed so that more than 12 in. (300 mm) of concrete is cast below the bar. Thus, in ACI 318-51, the equivalent development length, which is proportional to $1/\mu$, for a top bar was 42.8% longer than that for a bottom bar.

When ACI 318 introduced ultimate strength design in 1963, the same multiplier was used in the expressions for ultimate bond stress. ACI 318-71[28] replaced the traditional bond stress calculation with expressions for the calculation of development length and accounted for the top-bar effect by multiplying the development length of a top bar by 1.4.

AASHTO adopted the development-length specifications of ACI 318-71, including the 1.4 multiplier, in its 1979 interim specifications for bridges[29] and has maintained the 1.4 factor ever since.

The 1.4 ratio for bond between top bars and bottom bars was maintained by ACI 318 until the 1989 version, when the multiplier was reduced to 1.3. According to the commentary, this change was based largely on the findings by Jirsa and Breen[10] and Jeanty et al.[30]

Jirsa and Breen conducted pullout tests on large (72-in.-tall [1830 mm]) blocks of concrete with both anchored bars and spliced bars. In addition, constant-height beams were tested with splices near both the bottom and top surfaces. The primary variable in the study was the bar casting position. The test bars were arranged "so that the depth of concrete in the form below the bar was varied." In addition, the slump was varied from 3 in. to 8 ½ in. (75 mm to 216 mm).

Jirsa and Breen noted that "concrete slump is a very important variable in determining the effects of casting position." Their tests showed that when low-slump concrete was used, the equivalent top-bar factor was generally less than the 1.4 factor assumed by the then-current ACI and AASHTO codes. They proposed multipliers for top bars that were based on the following concrete slump ranges (less than 4 in. [100 mm], 4 in. to 6 in. [100 mm to 150 mm], and greater than 6 in. [150 mm]).

For concrete with a slump less than 4 in. (100 mm), the recommendation was for a top-bar multiplier ranging from 1.0 to 1.3, depending on the amount of concrete cast below the bar. For slumps of 4 in. to 6 in. (150 mm), the recommended multiplier ranged from 1.0 to 1.6, and for slumps greater than 6 in., the multiplier ranged from 1.0 to 2.2.

Jirsa and Breen specifically noted that the recommended multiplier values for slumps less than 4 in. (100 mm) be used in design "only when the designer is confident that the control over the concrete consistency in the field is sufficient to warrant its use."

It is interesting to note that ACI 318 adopted the reduced multiplier of 1.3, which was specifically recommended by Jirsa and Breen for slumps less than 4 in. (100 mm) when their data showed that the actual multiplier could be in excess of 2.0 when higher-slump concrete is used.

With few exceptions, most of the studies that evaluated the top-bar effect for mild steel reinforcement utilized constant-height specimens and varied the amount of concrete below the bar. Thus, in each of these studies the amount of concrete below the reinforcement was directly coupled with the corresponding amount of concrete above the bar. It is therefore plausible that many of the correlations that have historically been drawn about the dependence of bond on the amount of fresh concrete placed below the reinforcement would also hold true if based on the reciprocal amount (lack) of concrete above the reinforcement.

One experimental investigation, which specifically decoupled the top- and bottom-surface distances for deformed steel bars, was performed in the 1980s by Brettman, Darwin, and Donahey.[31] In this study, specimens were cast with varying overall heights and with varying distances of the reinforcement from the top and bottom surfaces. Furthermore, the study utilized concretes with varying fluidities to investigate the effect of high-range water-reducing admixtures on development length. The researchers noted that, contrary to conventional wisdom, their findings indicated "high-slump superplasticized concretes will give a lower bond strength than low- and medium-slump concretes of the same compressive strength." The researchers also noted that when high-range water-reducing admixtures are used, "the longer the concrete remains plastic the lower the bond strength."

Moreover, Brettman et al. had the following key findings pertaining to reinforcement placement: "A significant reduction in bond strength can occur for bars with less than 12 in. of concrete below the bar if the bars are top-cast (upper surface) bars." The researchers further stated that "a sharp drop-off in bond strength between bottom-cast bars and top-cast bars strongly suggests an upper surface effect, even for relatively low amounts of concrete below the bar," and recommended that the ACI top-bar requirements be applied to all top-cast bars. The researchers also recommended that the lowest-slump concrete that can be consolidated properly should be used to obtain the best

concrete-steel bond strength.

Most of the key findings pertaining to the effect of casting depth and fluidity on bond of straight reinforcing bars in tension have been summarized by ACI Committee 408 in the report ACI 408R-03.[32] This report notes that "most research indicates that while an increased depth of concrete below a bar reduces bond strength, the effect of shallow top cover is of greater significance." The report further states that the choice of 12 in. (300 mm) of concrete below a bar for the 30% increase in development length for top reinforcement is arbitrary.

Additionally, ACI 408R-03 notes that the bond strength of top-cast bars (bars near the upper surface of a concrete placement) appears to be especially sensitive to slump. The effect of concrete consistency (slump) on the bond strength of top-cast deformed bars was investigated by Zekany et al.[33] These researchers found that the bond of top-cast bars was decreased by as much as 40% to 50% when concrete slump was increased from 3 in. to 8 ½ in. (75 mm to 216 mm).

This PCI study finds that the top-strand effect in pretensioned members is primarily a function of the amount of concrete above the strand, which is in excellent agreement with the findings by Brettman et al., Zekany et al., and ACI 408R-03 for deformed bars. Also, the evidence that this effect becomes more pronounced with increasing concrete fluidity is in excellent agreement with the findings of Ferguson and Thompson, Jirsa and Breen, Brettman et al., Zekany et al., and ACI Committee 408.

(continued from page 97)

cess of 40 in. (1020 mm) ($80d_b$).

In the 4-in.-thick (100 mm) panel test series made with flowable concrete, specimen Le45 had an implied transfer length of 46 in. (1170 mm) ($88d_b$) and still withstood 92% of the nominal moment capacity as calculated by the Martin-Korkosz method. Specimen Le60 had an implied transfer length of 54 in. (1370 mm) ($103d_b$), more than twice the assumed value for transfer length, and was able to withstand 90% of the nominal moment capacity. However, it is uncertain if these members would have performed as well under long-term sustained loading.

Because the 4-in.-thick (100 mm) panel tests confirmed that end-slip measurements were good predictors of transfer length, the end-slip measurement technique described herein can be utilized by individual precast concrete producers to determine the extent of the top-strand effect with their own mixtures. Engineering managers at precasting plants A and B utilized this technique to implement design assumptions for their plants based on the performance of their own mixtures.

The findings of this study have significant implications for the design engineer, who may not always know the final casting orientation of the product that he or she is designing. The fact that there was a significant difference in the implied transfer lengths for upper and lower layers of pretensioned reinforcement in spandrels and wall panels (observed at plant B) suggests that there could be long-term serviceability issues, such as member bowing, that might be induced because of unequal prestress forces unknowingly introduced. In addition, if retarding admixtures are a contributing factor to the large top-strand effects noted for mix 3 and mix 4* flowable, then the top-bar effect could fluctuate significantly for a given mixture design as admixture dosages change to maintain concrete consistency at varying temperatures.

The significant reduction in bond capacity that typically results near the top surface of members with a high-fluidity concrete may be the primary reason that initial LBPTs conducted with SCC resulted in low pullout values compared with those using the recommended mixture by Logan, which typically has a slump of 3 in. to 4 in. (75 mm to 100 mm). In these pullout tests, strands are cast vertically so that a strand specimen has both top-cast and bottom-cast regions.

Considerable research is still needed to identify the contributing factors leading to the noted top-strand effect and to develop a methodology to reliably identify those mixtures and situations that will likely result in the significantly lower bonding capabilities noted herein.

RECOMMENDATIONS

The results of the current research emphasize the importance of casting position and concrete fluidity on strand bond. The following recommendations reflect these findings:

- Because strand end-slip measurements have been shown to be reliable predictors of transfer length, precasters should utilize this technique to determine the extent of the top-strand effect with their current mixtures when used in bond-critical applications.
- Design engineers should recognize that pretensioned strands located near the (as-cast) top surface of concrete members with high-fluidity concrete can have significantly longer transfer lengths and potentially longer development lengths than those suggested by both ACI[2] and AASHTO.[3] In lieu of obtaining mixture-specific data as recommended above, the approximations for average transfer-length values (presented in Fig. 36 and 37) representing members cast at six different PCI Producer Member plants could be used as an interim guide. These approximate relationships are restated here.

Bilinear approximation:

When $d_{cast} < 8$ in., $L_t = (90 - 5d_{cast})d_b$

When $d_{cast} \geq 8$ in., $L_t = 50d_b$

Stepped approximation:

When $d_{cast} < 4$ in., $L_t = 80d_b$

When 4 in. $\leq d_{cast} < 8$ in., $L_t = 65d_b$

When $d_{cast} \geq 8$ in., $L_t = 50d_b$

- In bond-critical applications with

strands located near the top casting surface and when the effect of casting depth on strand bond for existing mixtures is unknown, the lowest concrete slump that can be properly consolidated should be used.[14,31]

ACKNOWLEDGMENTS

The author sincerely appreciates the many individuals and companies who have assisted this work through financial contributions and technical expertise.

Major funding for this work is being provided by PCI and KDOT. The following companies are providing further funding: A. L. Patterson, American Spring Wire, Axim Italcementi Group, BASF Admixtures, Consulting Engineers Group, Coreslab Structures, Grace Construction Products, High Concrete Group, Metromont Corp., Molin Concrete Products, Shockey Precast Group, Sika Corp., Spancrete Industries, Strand-Tech Martin, Stresscon Corp., and Tindall Corp.

The author specifically thanks PCI for funding and administering a large portion of the work described herein and members of the PCI SCC Strand Bond Steering Committee and the Technical Review Committee for their valuable contributions during the development and execution of the research plan.

In addition, the author is extremely grateful to Kenneth Baur, PCI Fellow and director of research and development and technical sales support at High Concrete Structures in Denver, Pa. Baur served as chair of the PCI SCC Strand Bond Steering Committee and was invaluable in securing the financial support and collaboration necessary to complete this work. In addition, the author is thankful to the many individuals serving on the project steering committee. These members, listed in alphabetical order, are shown along with their respective organizations: Ken Baur, High Concrete Group; Harry Gleich, Metromont Corp.; Don Logan, Stresscon Corp.; Ed Mansky, Grace Construction Products; Ondrej Masek, Sika Corp.; Richard Miller, University of Cincinnati; Frank Nadeau, Tindall Corp.; Charles Nmai, BASF Admixtures; Andy Osborn, Wiss, Janney, Elstner Associates Inc.; Larbi Sennour, The Consulting Engineers Group Inc.; and Jim Wamelink, Axim Italcementi Group.

The author expresses appreciation to the members of the external technical review committee, established by the project steering committee, who provided valuable input in the determination of the research plan, especially in the selection of specimen sizes and reinforcing details, for the original test series. Members of the technical review committee are listed in alphabetical order: Roger Becker, Spancrete Industries; Bob Mast, Berger/ABAM Engineers Inc.; and Norm Scott, The Consulting Engineers Group Inc.

The author thanks the following PCI Producer Members (in alphabetical order) for donating specimens and allowing their production schedules to be interrupted in order to cast the specimens described herein: Coreslab Structures, Kansas City, Kans.; Coreslab Structures, Phoenix, Ariz.; High Concrete Structures, Denver, Pa.; Metromont Corp., Greenville, S.C.; and Spancrete Industries, Green Bay, Wis.

The author also thanks Dr. Kyle Larson, former graduate student at KSU, who greatly assisted me by traveling to the precasting facilities to help with form setup and instrumentation, determination of concrete properties, strand end-slip measurements, and data reduction from the original test series. Finally, the author thanks Matt Krick, project engineer at High Concrete Structures Inc. and Philip Barr and Justin Lamb, former engineering interns at one of the plants, for their painstaking work in preparing/cleaning strands and recording data.

NOTATION

d_b = diameter of strand
d_{cast} = strand depth from the top surface of concrete placement
L_d = development length
L_{tr} = transfer length
f_{ps} = stress in prestressed reinforcement at nominal strength
f_{se} = effective stress in prestressing strand after allowance for all prestress losses
f_{si} = initial stress in prestressing strand immediately after de-tensioning
Δ = strand end slip

REFERENCES

1. Interim SCC Guidelines FAST Team. 2003. *Interim Guidelines for the Use of Self-Consolidating Concrete in Precast/Prestressed Concrete Institute Member Plants*. 1st ed. Chicago, IL: Precast/Prestressed Concrete Institute (PCI).
2. ACI 318. 2005. *Building Code Requirements for Structural Concrete (ACI 318-05) and Commentary (ACI 318R-05)*. Farmington Hills, MI: American Concrete Institute (ACI).
3. American Association of State Highway and Transportation Officials (AASHTO). 2007. *AASHTO LRFD Bridge Design Specifications*. 4th ed. Washington, DC: AASHTO.
4. Russell, B. W., and N. H. Burns. 1993. Design Guidelines for Transfer, Development and Debonding of Large Diameter Seven Wire Strands in Pretensioned Concrete Girders. Research project 3-5-89/2-1210, Texas Department of Transportation.
5. Peterman, R. J., J. A. Ramirez, and J. Olek. 2000. Influence of Flexure-Shear Cracking on Strand Development Length in Prestressed Concrete Members. *PCI Journal*, V. 45, No. 5, (September–October): pp. 76–94.
6. Clark, A. P. 1946. Comparative Bond Efficiency of Deformed Concrete Reinforcing Bars. *ACI Journal*, V. 43, No. 4 (December): pp. 381–400.
7. Clark, A. P. 1950. Bond of Concrete Reinforcing Bars. *ACI Journal*, V. 46, No. 3 (November): pp. 161–184.
8. Menzel, Carl A. 1952. *Effect of Settlement of Concrete on Results of Pullout Tests.* Research department bulletin no. 41. Skokie, IL: Portland Cement Assocation.
9. Ferguson, P. M., and J. N. Thompson. 1962. Development Length for Large High Strength Reinforcing Bars in Bond. *ACI Journal*, V. 59, No. 7 (July): pp. 887–922.
10. Jirsa, J. O., and J. E. Breen. 1981. Influence of Casting Position and Shear on Development and Splice Length—Design Recommendation. Research report no. 242-3F, Center for Transportation Research, University of Texas at Austin.
11. Buckner, D. 1995. A Review of Strand Development Length for Pretensioned Concrete Members. *PCI Journal*, V.

40, No. 2 (March–April): pp. 84–105.

12. Petrou, M. F., and W. S. Joiner. 1996. *Continuing Investigation of Strand Slippage in 24 Inch Octagonal Prestressed Concrete Piles*. Publication no. FHWA-SC-96-04. Columbia, SC: University of South Carolina.

13. Petrou, M. F., and W. S. Joiner. 2000. Excessive Strand Slip in Prestressed Piles. *ACI Structural Journal*, V. 97, No. 5 (September–October): pp. 774–782.

14. Wan, B., M. F. Petrou, K. A. Harries, and A. A. Hussein. 2002. Top Bar Effects in Prestressed Concrete Piles. *ACI Structural Journal*, V. 99, No. 2 (March–April): pp. 208–214.

15. Wan, B., K. A. Harries, and M. F. Petrou. 2002. Transfer Length of Strands in Prestressed Concrete Piles. *ACI Structural Journal*, V. 99, No. 5 (September–October): pp. 577–585.

16. Lane, Susan N. 1998. *A New Development Length Equation for Pretensioned Strands in Bridge Beams and Piles*. Publication no. FHWA-RD-98-116. Washington, DC: Federal Highway Administration.

17. AASHTO. 2004. *AASHTO LRFD Bridge Design Specifications*. 3rd ed. Washington, DC: AASHTO.

18. Logan, Donald R. 1997. Acceptance Criteria for Bond Quality of Strand for Pretensioned Prestressed Concrete Applications. *PCI Journal*, V. 42, No. 2 (March–April): pp. 52–90.

19. Brooks, Mark D., K. H. Gerstle, and D. R. Logan. 1988. Effect of Initial Strand Slip on the Strength of Hollow-Core Slabs. *PCI Journal*, V. 33, No. 1 (January–February): pp. 90–111.

20. Anderson, A. R., and R. G. Anderson. 1976. An Assurance Criterion for Flexural Bond in Pretensioned Hollow-Core Units. *ACI Journal* V. 73, No. 8 (August): pp. 457–464.

21. Industry Handbook Committee. 2004. *PCI Design Handbook: Precast and Prestressed Concrete.* 6th ed. Chicago, IL: PCI.

22. Barnes, R. W., J. W. Grove, and N. H. Burns. 2004. Experimental Assessment of Factors Affecting Transfer Length. *ACI Structural Journal*, V. 100, No. 6 (November–December): pp. 740–748.

23. Oh, B. H., and E. S. Kim. Realistic Evaluation of Transfer Lengths in Pretensioned, Prestressed Concrete Members. *ACI Structural Journal*, V. 97, No. 6 (November–December): pp. 821–830.

24. Larson, K., R. Peterman, and H. Rasheed. 2005. Strength-Fatigue Behavior of FRP Strengthened Prestressed Concrete T-Beams. *ASCE Journal of Composites for Construction,* V. 9, No. 4 (July–August): pp. 313–326.

25. Buettner, D., and R. Becker. 1998. *Manual for the Design of Hollow Core Slabs.* 2nd ed., pp. 2-19 through 2-22. Chicago, IL: PCI.

26. Martin, Leslie D., and Walter J. Korkosz. 1995. Strength of Prestressed Concrete Members at Sections Where Strands Are Not Fully Developed. *PCI Journal*, V. 40, No. 5 (September–October): pp. 58–66.

27. ACI 318. 1951. *Building Code Requirements for Reinforced Concrete (ACI 318-51).* Farmington Hills, MI: ACI.

28. ACI 318. 1971. *Building Code Requirements for Reinforced Concrete (ACI 318-71).* Farmington Hills, MI: ACI.

29. AASHTO Subcommittee on Bridges and Structures. 1979. *Interim Specifications, Bridges.* Washington, DC: AASHTO.

30. Jeanty, P. R., D. Mitchell, and M. S. Mirza. 1988. Investigation of 'Top Bar' Effects in Beams. *ACI Structural Journal*, V. 85, No. 3. (May–June): pp. 251–257.

31. Brettmann, B. B., D. Darwin, and R. C. Donahey. 1986. Bond of Reinforcement to Superplasticized Concrete. *ACI Journal*, V. 83, No. 1 (January–February): pp.98–107.

32. ACI 408. 2003. *Bond and Development of Straight Reinforcing Bars in Tension*. ACI 408R-03. Farmington Hills, MI: ACI.

33. Zekany, A. J., S. Neumann, J. O. Jirsa, and J. E. Breen. 1981. The Influence of Shear on Lapped Splices in Reinforced Concrete. Research report 242-2, Center for Transportation Research, Bureau of Engineering Research, University of Texas at Austin.

34. Khayat, K. H. 1998. Use of Viscosity-Modifying Admixture to Reduce Top-Bar Effect of Anchored Bars Cast with Fluid Concrete. *ACI Materials Journal*, V. 95, No. 2 (March–April): pp. 158–167.

35. Attiogbe, E. K., H. T. See, and J. A. Daczko. 2002. Engineering Properties of Self-Consolidating Concrete. In *Proceedings of the First North American Conference on the Design and Use of Self-Consolidating Concrete*. Chicago, IL: Northwestern University.